Adaptive remodeling of rat adrenomedullary stimulus-secretion coupling in a chronic hypertensive environment

Vincent Paillé, Joohee Park, Bertrand Toutain, Jennifer Bourreau, Pierre Fontanaud, Frédéric de Nardi, Claudie Gabillard-Lefort, Dimitri Bréard, David Guilet, Daniel Henrion, et al.

Cellular and Molecular Life Sciences (2025) 82:31
https://doi.org/10.1007/s00018-024-05524-5

ORIGINAL ARTICLE

Adaptive remodeling of rat adrenomedullary stimulus-secretion coupling in a chronic hypertensive environment

Vincent Paillé[1,2] · Joohee Park[1] · Bertrand Toutain[1] · Jennifer Bourreau[1] · Pierre Fontanaud[3] · Frédéric De Nardi[1] · Claudie Gabillard-Lefort[1] · Dimitri Bréard[4] · David Guilet[4] · Daniel Henrion[1] · Christian Legros[1] · Nathalie C. Guérineau[1,5]

Received: 1 February 2024 / Revised: 8 November 2024 / Accepted: 22 November 2024

Abstract

Chronic elevated blood pressure impinges on the functioning of multiple organs and therefore harms body homeostasis. Elucidating the protective mechanisms whereby the organism copes with sustained or repetitive blood pressure rises is therefore a topical challenge. Here we address this issue in the adrenal medulla, the master neuroendocrine tissue involved in the secretion of catecholamines, influential hormones in blood pressure regulation. Combining electrophysiological techniques with catecholamine secretion assays on acute adrenal slices from spontaneously hypertensive rats, we show that chromaffin cell stimulus-secretion coupling is remodeled, resulting in a less efficient secretory function primarily upon sustained cholinergic challenges. The remodeling is supported by revamped both cellular and tissular mechanisms. This first includes a decrease in chromaffin cell excitability in response to sustained electrical stimulation. This hallmark was observed both experimentally and in a computational chromaffin cell model, and occurs with concomitant changes in voltage-gated ion channel expression. The cholinergic transmission at the splanchnic nerve-chromaffin cell synapses and the gap junctional communication between chromaffin cells are also weakened. As such, by disabling its competence to release catecholamines in response sustained stimulations, the hypertensive medulla has elaborated an adaptive shielding mechanism against damaging effects of redundant elevated catecholamine secretion and associated blood pressure.

Keywords Chromaffin cell excitability · Cholinergic synaptic transmission · Gap junctional coupling · Acute adrenal slices · Catecholamine assays · Hypertensive rats · Voltage-gated ion channels · Nicotinic receptors

Introduction

A rise in circulating catecholamine (CA) levels is a crucial step triggered by the organism to cope with a stressful situation. By releasing both epinephrine (E) and norepinephrine (NE), the adrenal medullary tissue crucially contributes to this response. Beyond the beneficial effect of CA secretion elicited by an acute stress, sustained and/or repetitive CA secretion episodes (in response to chronic stressful situations for example) can have deleterious outcomes [1], as unveiled by the elevated blood pressure observed in response to chronic infusion of E in rat [2, 3] or in chronically cold stressed rats [4]. It has long been reported that increased blood pressure is associated with a sympathetic nervous system hyperactivity leading to a raised neural tone [5, 6] and increased plasma E and NE [7]. The adrenal medulla being the unique source of circulating E, this assigns the secretory function of the medulla and more

✉ Nathalie C. Guérineau
nathalie.guerineau@igf.cnrs.fr

1 Univ Angers, INSERM, CNRS, MITOVASC, Équipe CARME, SFR ICAT, F-49000 Angers, France

2 Nantes Université, INRAE, UMR 1280, PhAN, Nantes, France

3 Institut de Génomique Fonctionnelle, Université Montpellier, CNRS, INSERM, Montpellier, France

4 Univ Angers, SONAS, SFR QUASAV, F-49000 Angers, France

5 Institut de Génomique Fonctionnelle, Université Montpellier, CNRS, INSERM, Montpellier, France

Published online: 27 December 2024

generally the sympatho-adrenal axis as critical determinants of arterial hypertension pathogenesis [8–10]. Reciprocally, although it is indisputable that the adrenal medulla primarily contributes to enhance blood pressure, how the adrenal secretory function copes with a chronic hypertensive environment remains elusive. Based on the notion of homeostasis, the basis of survival for any living organism, it is reasonable to propose that compensatory mechanisms occur to protect the organism against the deleterious effects of a chronic increase in blood CA levels, thus positioning these mechanisms as a consequence of hypertension rather than a cause. We addressed this issue in an animal model of chronic hypertension, the spontaneously hypertensive rat. In this model, the circulating E levels gradually increase as arterial hypertension develops and then stabilize in adults to become comparable to those in age-matched normotensive rats [11]. Consistent with our working hypothesis, this suggests that the adrenal gland develops protective and/or compensatory mechanisms dedicated to normalize blood CA levels. To date nothing is known on the adaptive mechanisms elaborated by the neuroendocrine chromaffin cells to adjust the release of CA.

Adrenal CA secretion and more generally the adrenomedullary tissue function are controlled by the coordination of interconnected and complex pathways [12]. The initial incoming command comes from the sympathetic nervous system that releases mainly acetylcholine (ACh) but also neuropeptides (PACAP, VIP...) at splanchnic nerve terminals synapsing onto chromaffin cells [13, 14]. The resulting ACh-evoked chromaffin cell depolarization and subsequent cytosolic Ca^{2+} rise are key processes for CA exocytosis. In addition and unraveled from studies in both acute adrenal slices and in vivo in anaesthetized rodents, the local communication mediated by gap junctions between chromaffin cells represents a functional route by which biological signals propagate between adjacent cells and subsequently contribute to CA release [15–20].

To elucidate the feedback mechanisms elaborated by the adrenal medullary tissue to manage a chronic sustained elevated blood pressure, we investigated chromaffin cell stimulus-secretion coupling in acute adrenal slices of adult spontaneously hypertensive rats (SHRs) and their parent age-matched normotensive Wistar Kyoto (WKY) rats. By driving numerous cellular/tissular processes, chromaffin cell excitability is a major player in stimulus-secretion coupling. It relies on intricate mechanisms, not only supported by ion channels expressed at the plasma membrane, but also by the crosstalk between cholinergic and peptidergic innervation [21] and the gap junctional electrical coupling between chromaffin cells [17, 19, 20]. We identified relevant modifications in chromaffin cell excitability through changes in voltage-gated ion channel expression, cholinergic synaptic neurotransmission and gap junctional communication, that argue for a less efficient stimulus-secretion coupling in hypertensive animals, markedly observed upon robust challenges. We propose that this functional plasticity reflects an adaptive shielding mechanism, avoiding the detrimental effects of sustained or repetitive huge CA secretion episodes. More generally, this study describes novel adaptive mechanisms that take place in the medullary tissue and how they act in a coordinated manner to dampen CA release.

Materials and methods

Ethical approval and animals: Animals were housed in groups of 3–4 par cages (standard sizes according to the European animal welfare guidelines 2010/63/EU) and maintained in a 12 h light/dark cycle, in stable conditions of temperature (22 °C) and humidity (60%). Food and water were provided *ad libitum*. All procedures in this study also conformed to the animal welfare guidelines of the European Community and were approved by the French Agriculture and Forestry Ministry (authorization numbers/licences 49-2011-18, 49–247, A49007002 and D44015) and by the regional ethic committee (authorization CEEA.2011.12 and APAFIS#2017072117413637).

Data were collected from 16- to 20-week-old spontaneously hypertensive male rats (SHRs) and from their control age-matched normotensive male Wistar-Kyoto (WKY) rats (SHR/KyoRj and WKY/KyoRj, Janvier Labs, Le Genest-St-Isle, France). At this age, SHRs exhibited an established increase in arterial blood pressure compared to WKY rats [22]. To control the hypertensive/normotensive state of the animals, systolic and diastolic blood pressures (SBP and DBP, respectively) were measured by tail-cuff plethysmography in awake SHRs and WKY rats. Heart rhythm was also monitored. For 3 weeks prior to data collection, the rats were trained to measure blood pressure (one session every 3–4 days, each session consisting of 10 successive measurements at 2-min intervals). The measurements taken into account were those collected on the last day of habituation, and an average value of the 10 measurements was calculated for each rat. As expected, systolic blood pressure was significantly higher in SHR (200.7 ± 31.7 mmHg, $n = 11$ *versus* 163.5 ± 22.4 mmHg, $n = 11$ in WKY rats, $p = 0.0031$, one-tail Mann-Whitney test). Diastolic pressure was also higher in SHRs (145.2 ± 41.9 mmHg, $n = 11$ *versus* 111.5 ± 41.4 mmHg, $n = 11$ in WKY rats, $p = 0.0314$, one-tail Mann-Whitney test). For each animal, mean arterial pressure (MAP) was calculated from systolic and diastolic pressure values, using Gauer's formula, as follows $MAP = DBP + [(SBP - DBP)/3]$) [23, 24]. SHRs exhibited a significant increase in MAP compared to WKY rats (163.6 ± 37.0

mmHg, $n=11$ *versus* 128.9 ± 33.9 mmHg, $n=11$, respectively, $p=0.0168$, one-tail Mann-Whitney test). Heart rate is also increased in SHRs (378.4 ± 21.6 beats/min, $n=11$ *versus* 321.3 ± 41.0 beats/min, $n=11$ in WKY rats, $p=0.0017$, Mann-Whitney test). The body weight did not significantly differ between SHRs (401.4 ± 33.3 g, $n=38$) and WKY rats (417.2 ± 43.6 g, $n=47$, $p=0.0689$, unpaired t test, Figure S1A). As a consequence of the arterial hypertension, the heart weight was statistically higher in SHRs (1.51 ± 0.23 g, $n=38$ *versus* 1.22 ± 0.10 g, $n=47$ in WKY rats, $p<0.0001$, unpaired t test, Figure S1B). Accordingly, the heart/body weight ratio (x100) was also significantly higher in SHRs (0.38 ± 0.06, $n=38$ *versus* 0.29 ± 0.02, $n=47$ in WKY rats, $p<0.0001$, unpaired t test, Figure S1C).

Adrenal slice preparation

Acute slices from SHRs and WKY rats were prepared as described [15, 25]. Briefly, after removal, the adrenal glands were kept in ice-cold saline for 2 min. Before slicing, a gland was desheathed of the surrounding fat tissue and was next glued onto an agarose cube and transferred to the stage of a vibratome (HM 650 V vibrating blade microtome, Microm Microtech, Francheville, France). Slices (200 µm thickness for the electrophysiological recordings and 150 µm thickness for CA secretion assay) were cut with a razor blade and transferred to a storage chamber maintained at 37 °C, containing Ringer's saline (in mM): 130 NaCl, 2.5 KCl, 2 $CaCl_2$, 1 $MgCl_2$, 1.25 NaH_2PO_4, 26 $NaHCO_3$, 12 glucose and buffered to pH 7.4. The saline was continuously bubbled with carbogen (95% O_2/5% CO_2).

Electrophysiology

All electrophysiological recordings were performed in acute slices. Adrenal slices were transferred to a recording chamber attached to the stage of a real-time confocal laser scanning microscope (LSM 5Live, Zeiss) equipped with an upright microscope (Axio Examiner, Zeiss, Le Pecq, France) and continuously superfused with Ringer's saline at 34 °C. All experiments were performed using the patch-clamp technique and electrophysiological signals were acquired using an EPC-10 USB Quadro patch-clamp amplifier (HEKA Electronik, Lambrecht/Pfalz, Germany) and PATCHMASTER software. Signals were sampled at 10 kHz and analyzed with FITMASTER (HEKA Electronik, Germany) and Igor Pro 7 (version 7.02, WaveMetrics Inc., Lake Oswego, OR). Ag/AgCl pellet was used as a reference ground electrode. For whole-cell recordings, pipettes were pulled from borosilicate glass and filled with the following internal solution (in mM): 140 potassium (K)-gluconate, 5 KCl, 2 $MgCl_2$, 1.1 EGTA, 5 Hepes, 4 MgATP, 0.3 NaGTP and titrated to pH 7.2 with KOH. Osmolarity was adjusted at 295 mOsm with K-gluconate and pipette resistance was 5-8MΩ. Voltage was corrected for the junction potential of about 13 mV. Pipette and cell capacitances were fully compensated and the series resistance was compensated at 75–80%. Membrane potential was recorded in the current-clamp mode and filtered at 3 kHz. The AP properties were examined by injecting current pulses of 500 ms duration from − 50 to + 60 pA at 1 Hz. The analysis of evoked APs was done using Mini Analysis software (Synaptosoft Inc. Fort Lee, NJ, USA).

For extracellular recordings of spontaneous AP currents in the loose-patch configuration, pipettes were pulled to a resistance of 5–10 MΩ when filled with the following saline (in mM): 130 NaCl, 2.5 KCl, 2 $CaCl_2$, 1 $MgCl_2$, 10 HEPES, 10 glucose and buffered to pH 7.4 with NaOH. Osmolarity was adjusted at 295 mOsm with NaCl. The liquid junction potential was approximately 0 mV. Once the tip of the pipette was positioned at the surface of a chromaffin cell, a minimal suction pressure was applied (seal resistance < 500 MΩ) and the electrical activity was recorded in the voltage-clamp mode (0 mV) of the loose cell-attached configuration [26]. This method allows investigation of membrane excitability under physiological conditions and stable recordings of firing rate can therefore be obtained [27, 28]. APs were detected by a threshold method based on calculation of the median absolute deviation (MAD) [29], by using Igor Pro 7 software (version 7.02). This method provides an unbiased estimate of the standard deviation (SD) of background noise. Briefly, the absolute value of the deviation from the mean of the potential values is calculated and the median of this deviation (MAD) is determined. MAD divided by the 75th percentile of the standard normal distribution equals the SD of the background noise. By applying a coefficient of 4 to the SD value, we can reliably and reproducibly separate APs from background noise. The analysis of the discharge pattern was performed on the spontaneous electrical activity of cells recorded in either whole-cell or loose patch configuration. To discriminate between a regular and a bursting pattern, the regularity of the firing discharge was investigated by calculating the coefficient of variation (CV) of inter-spike interval (ISI) distribution. A regular firing mode is associated with a CV < 1 and a bursting mode with a CV > 1, as described [30]. Regarding the extracellular experiments with PACAP, after a 2–5 min resting period, we initiated recordings for 5 min (control condition). Using a Pressurized Drug Applicator (NPI electronic, Bauhofring, Germany) attached to a glass pipette, PACAP was then puffed near the recorded cell for 5 min (PACAP condition). The results were represented as a

percentage of the AP frequency following PACAP application relative to the control condition. Three different doses of PACAP were used (0.1, 1 and 10 µM) on distinct slices and chromaffin cells. Spontaneous excitatory postsynaptic currents (sEPSCs) were recorded in chromaffin cells voltage-clamped at -80 mV and were filtered at 1 kHz, as previously described [31]. To increase the percentage of chromaffin cells exhibiting sEPSCs, recordings were performed by applying a 80 mM KCl puff at the vicinity of the recording cells [32, 33]. In some cells, a quantal analysis of sEPSCs was performed. Only single events were selected for construction of amplitude histograms. The histograms were inspected for the presence of peaks and a corresponding number of Gaussians was then fitted by nonlinear regression using GraphPad Prism 5.0 software (San Diego, USA). Quantal size was estimated from the mean value of the first Gaussian curve fitted to the amplitude distribution histogram. Normalized sEPSC decays were fitted by a single exponential using the Simplex fit algorithm based on the sum of squared errors SSE. Only fits with a SSE < 0.001 were taken into consideration. The analysis was done using Mini Analysis software.

Mathematical model of chromaffin cell electrical firing

Chromaffin cell electrical activity was modeled using the chromaffin cell simulation developed by Warashina and Ogura [34]. The computational model was adapted to the JSim software [35], available at https://www.imagwiki.nibib.nih.gov/physiome/jsim. The time adaptive integration using the Radau method (dt = 0.01 ms) was used to give stable solutions to ordinary differential equations. Conductance changes between SHRs and WKY rats were extrapolated from the changes observed in the expression level of the most abundant transcript for Na^+, Ca^{2+} and Ca^{2+}-dependent K^+ channels, that are $Na_V1.3$ (1.4-fold change), $Ca_V1.3$ (2-fold change) and KCa1.1/KCa2.3 (1.7-fold change).

Dye transfer assay. The fluorescent dye LY (Lucifer yellow-CH, dilithium salt, 1 mM in internal solution) was introduced into chromaffin cells using patch pipettes. The probability of LY diffusion was expressed as a ratio corresponding to the number of injected cells that show dye transfer to adjacent cells over the total number of injected cells, as previously described [36]. Cells were viewed with a 63x/1.0 NA Plan-Apochromat water immersion objective (Zeiss). Dye transfer between gap junction-coupled cells was imaged with a real-time confocal laser-scanning microscope (LSM 5Live, Zeiss) equipped with a diode laser 488 nm (100 mW). The extent of LY diffusion was estimated by counting the number of neighboring cells that received dye in 15 min.

Quantification of mRNA expression levels by real-time PCR

Total RNA was extracted from macrodissected adrenal medulla using the RNeasy® Micro extraction kit (Qiagen, Courtaboeuf, France), as previously described [18]. RNA (500 ng) was first reverse transcribed using the QuantiTect® Reverse Transcription kit (Qiagen) in a final volume of 10 µl. Real-time PCR analyses of the target genes and the reference genes *Gusb*, *Hprt* and *Gapdh* were performed using Sybr® Green PCR master mix (Applied Biosystems, Foster City, CA) with 1:100 of the reverse-transcription reaction, and were carried out on an ABI 7500 SDS Real-Time PCR system (Applied Biosystems). After an initial denaturation step for 10 min at 95 °C, the thermal cycling conditions were 40 cycles at 95 °C for 15 s and 60 °C for 1 min. Specificity of amplification was checked by melting curve analysis. Each sample value was determined from duplicate measurements. Expression of the target transcripts was normalized to the mean of the expression level of the three reference genes according to the formula $E = 2^{-(Ctmean[Target]-Ctmean[Reference])}$, where Ctmean is the mean threshold cycle. The fold difference values were determined according to Livak's method [37]. Primer sequences of target genes are given in Table S3 and the concentration used was 300 nM for all genes.

Determination of Cx43 and ZO-1 protein expression. Cx43 and ZO-1 expression levels were achieved on macrodissected adrenal medulla (5 SHRs and 5 WKY rats). After decapsulation, the medullary tissue was separated from the cortex, quickly frozen and pulverized in liquid nitrogen. For each animal the right and the left medulla were pooled in a same sample. The samples were resuspended in lysis buffer (10 mM Tris-HCl, pH 7.4, 1 mM sodium orthovanadate, 10 mM NaF as phosphatase inhibitors and 1% SDS), supplemented with Mini complete protease inhibitors (Roche Applied Science, Laval, Quebec). The extracts were incubated 30 min at 4 °C, sonicated and centrifuged for 20 min at 12,000 g. The supernatant was then collected, and the protein concentration was determined using the Pierce BCA Protein Assays Kit (Thermo Fisher Scientific, Rockford, IL) Protein samples (25 µg) were separated by 10% SDS-PAGE (4–15% gradient for ZO-1 detection). Electrophoresed proteins were transferred onto a nitrocellulose membrane. Blots were then blocked with 5% milk in TBS (pH 7.4, 0.1% Tween 20) for 1 h at room temperature with gentle agitation. Blots were next incubated with polyclonal antibodies, a rabbit anti-Cx43 (1:500, Thermo Fisher Scientific) or a rabbit

anti-ZO-1 (1:250, Thermo Fisher Scientific) in TBS-Tween 0.1% containing 5% milk, at 4 °C overnight. Following washout, blots were incubated with secondary antibodies peroxydase conjugated for 1 h at room temperature. Proteins were visualized with a LAS-3000 imager (Fuji) using an ECL-Plus Chemiluminescence kit (Thermo Fisher Scientific). To ensure equal loading of protein samples, blots were stripped of connexin or ZO-1 antibodies and reprobed with an actin-specific monoclonal antibody (β-actin, 1:5000, Sigma). Intensities of Cx43 and ZO-1 bands were normalized to those of actin and quantified using the Las-3000 software.

CA assays from adrenal slice supernatants

Chromaffin cell ability to secrete CA was assessed by monitoring E and NE released in slice supernatant, as previouly described [38]. After a 5-min basal (B) condition, slices were challenged (S) with either ACh-containing saline or Ringer saline, during 5 min. For each slice, results were expressed as the stimulation ratio S/B. To calculate basal or stimulated amounts of secreted E and NE, the medulla surface was estimated for each slice. To achieve this, at the end of experiments, slices were bathed for 2 min in hematoxyline (1 g/l). The differential staining intensity between cortex and medulla allowed estimating the medulla surface, on the two slice faces. The volume was then subsequently calculated. After collection, samples were kept at -20 °C during 2–3 days before use. E and NE were assayed by High Performance Liquid Chromatography (HPLC). A benzylamine pre-column derivatization was used to generate fluorescent benzoxazole derivatives [39], which were next separated by C18 reversed-phase HPLC (Vydac 218TP54 column, 5 mm, 4.6 mm i.d. x 250 mm; Waters Separations Module 2695; multiwavelength fluorescence detector Waters 2475) [40]. The derivatization reactions were carried out using 20 µl of a standard solution of CA (L-epinephrine- and L-norepinephrine-L-bitartrate salts) or supernatant samples or water (blank) mixed to benzylamine (50 mM) and 3-cyclohexylaminopropanesulfonic acid (3.3 mM, pH 11) and potassium hexacyanoferrate III (1.7 mM). The resulting mixtures were incubated at 50 °C for 20 min and 20 µl were loaded onto the reverse phase C18-column. Isocratic elution was performed with a mobile phase consisting of 10 mM acetate buffer (pH 5.5) and acetonitrile (65/35, v/v) run at 1 ml/min. The column temperature was maintained at 23 °C. The detection was monitored at an excitation wavelength of 345 nm and an emission wavelength of 480 nm. To determine E and NE concentrations, the areas under the peaks of samples were compared to the peaks of the standard range used as external calibrator.

Solutions and chemicals

Benzylamine, 3-cyclohexylaminopropanesulfonic acid, potassium hexacyanoferrate III, L-epinephrine-L-bitartrate salt, L-norepinephrine-L-bitartrate salt, acetonitrile, Lucifer yellow (dilithium salt), pituitary adenylate cyclase activating polypeptide-38 (PACAP-38) and acetylcholine chloride were purchased from Sigma-Aldrich (Saint-Quentin Fallavier, France).

Statistical analysis

Statistics were performed with Prism 9 (version 9.4.1, GraphPad, San Diego, CA). Numerical data are expressed as the mean ± standard deviation. Differences between groups were assessed by using the non-parametric Mann-Whitney test. Unpaired Student's t-test was used to compare means when appropriate. The non-parametrical Wilcoxon matched-pairs signed-rank test was used to compare two related samples or to compare a single sample to a theoretical value (1 or 100%). For comparisons of more than two groups, the non-parametric Kruskal-Wallis test was used. The Spearman's rank correlation coefficient ρ was used to measure the relationship between paired data. Percentages were compared using a contingency table and the chi-square test or the Fisher's exact test when appropriate. Differences with $p < 0.05$ were considered significant, with *, $p < 0.05$, **, $p < 0.01$, ***, $p < 0.001$ and ****, $p < 0.0001$.

Results

Impaired CA release evoked by high ACh concentration in hypertensive rats

The competence of WKY and SHR chromaffin cells to secrete CA was investigated by assaying basal and ACh-evoked epinephrine (E) and norepinephrine (NE) released from acute slices (Fig. 1A, B and C). We took advantage of making slices from the two adrenals to estimate the medulla volume of the right and left glands for both SHRs and WKY rats, as previously reported [38]. For each rat, whether WKY or SHR, no difference was observed between the right and the left glands (0.85 ± 0.08 mm^3, $n = 4$ and 0.95 ± 0.15 mm^3, $n = 4$ for the right and left WKY glands, respectively, $p = 0.125$, and 1.17 ± 0.33 mm^3, $n = 4$ and 1.25 ± 0.32 mm^3, $n = 4$ for the right and left SHR glands, respectively, $p = 0.125$, Wilcoxon matched-pairs signed-rank test, Figure S1D). However, medullary tissue volume was significantly greater in SHRs (1.21 ± 0.30 mm^3, $n = 8$ glands for SHRs *versus* 0.90 ± 0.12 mm^3, $n = 8$ glands for WKY rats, $p = 0.0351$, Mann-Whitney test, Figure S1E). To

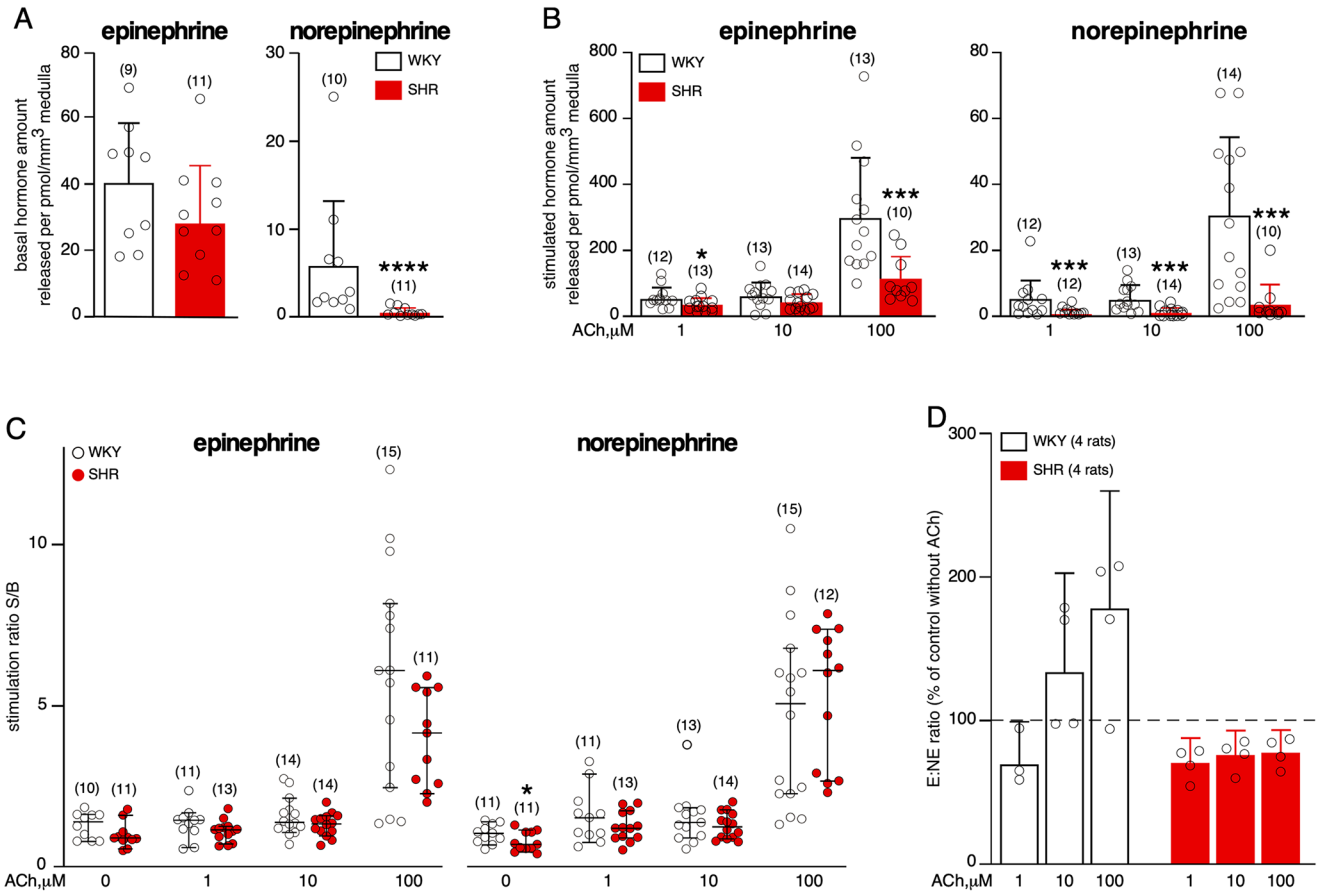

Fig. 1 Reduced competence to release CA in SHRs in response to robust ACh challenge. Acute adrenal slices from SHRs and WKY rats were incubated first for 5 min (basal (**B**) conditions) and then challenged (stimulated (S) conditions) with either ACh-containing saline or Ringer saline, during 5 min. Secreted epinephrine (**E**) and norepinephrine (NE) were assayed by HPLC. **(A)** Basal CA secretion (values and error bars represent mean and SD, $n=9$–11 slices, Mann-Whitney test, ****, $p<0.0001$). **(B)** CA secretion in response to increasing ACh stimulations. Both basal and ACh-evoked NE amounts released per mm^3 of medulla are significantly reduced in SHRs. Regarding E, amounts released per mm^3 medulla are mostly decreased in response to a high ACh concentration (100 µM)-evoked challenge. Values and error bars represent mean and SD ($n=10$–14 slices, Mann-Whitney test, *, $p<0.05$ and ***, $p<0.001$). **(C)** No difference in stimulation ratios S/B, indicating that the tissue responsiveness is preserved in SHRs. Values and error bars represent mean and SD ($n=10$–15 slices, Mann-Whitney test, *, $p<0.05$). **(D)** E:NE ratios calculated from the two adrenals pooled for each rat. Constant E:NE ratios in SHRs, contrasting with a progressive increase in E:NE in WKY rats, upon exposure to increasing concentrations of ACh. Values and error bars represent mean and SD ($n=4$ WKY rats and 4 SHRs, Kruskal-Wallis test, $p>0.05$)

make appropriate comparisons between SHRs and WKY rats, CA secretion was normalized per mm^3 medulla, as previously described [38]. The larger volume of the adrenal medullary tissue in SHRs (1.4 times) was taken into account in the normalization procedure. Under basal conditions, SHR chromaffin cells secreted 11.8-fold less NE than WKY cells (0.5 ± 0.5 pmol/mm^3, $n=11$ slices for SHRs *versus* 5.9 ± 7.4 pmol/mm^3, $n=10$ slices for WKY rats, $p<0.0001$, Mann-Whitney test, Fig. 1A, right graph). No change was observed for released E amounts (28.1 ± 17.0 pmol/mm^3, $n=11$ slices for SHRs *versus* 40.0 ± 18.3 pmol/mm^3, $n=9$ slices for WKY rats, $p=0.201$, Mann-Whitney test, Fig. 1A, left graph). Likewise, a significant decrease in NE release in SHRs was observed in response to ACh stimulations, both at low (1 µM) and high (10–100 µM) concentrations (Fig. 1B, $p=0.0007$, 0.0003 and 0.0002 for ACh 1, 10 and 100 µM, respectively, Mann-Whitney test). The E release amount was also significantly decreased, mostly at 100 µM ACh ($p=0.0160$, 0.0683 and 0.0005 for ACh 1, 10 and 100 µM, respectively, Mann-Whitney test). To go further, we investigated the ability of chromaffin cells to be stimulated by ACh. Irrespective to ACh concentrations (1-100 µM), the stimulation ratio was similar between SHRs and WKY rats, even at high ACh concentration (Fig. 1C, for E: x5.9 ± 3.5 ($n=15$ slices) and x4.0 ± 1.5 ($n=11$ slices) for WKY rats and SHRs, respectively, $p=0.1447$, Mann-Whitney test and for NE: x4.9 ± 2.9 ($n=15$ slices) and x5.3 ± 2.1 ($n=12$ slices) for WKY rats and SHRs, respectively, $p=0.3406$, Mann-Whitney test). Strengthening a deficiency in ACh-induced CA secretion in SHRs, the E:NE ratio remained

constant upon challenging SHR chromaffin cells with increasing ACh concentrations ($p = 0.7061$, $n = 4$ rats, Kruskal-Wallis test), while it gradually increased in WKY rats (Fig. 1D), as expected for ACh-induced CA secretion in a dose-dependent manner and preferential release of E over NE release, especially for high ACh concentration [38]. Altogether, this indicates that despite a preserved ability to release CA, stimulus-secretion coupling of chromaffin cells may be less efficient in SHRs. Aiming at identifying which element(s) of the adrenal stimulus-secretion is (are) altered in SHRs, we next performed a series of experiments focused on (i) chromaffin cell excitability, (ii) the cholinergic neurotransmission at the splanchnic nerve ending-chromaffin cell synapse and (iii) the gap junction-mediated communication between chromaffin cells.

Altered action potential firing in SHRs in response to sustained stimulations

Regarding the passive electrical membrane properties of chromaffin cells, significant changes were observed between SHRs and WKY rats for input resistance and capacitance (Table S1), predicting a plausible stimulus-secretion coupling reshaping in SHRs. To investigate chromaffin cell excitability under experimental conditions as close to in situ conditions as possible, spontaneous action potential (AP) firing at resting membrane potential was recorded in the loose cell-attached configuration (Fig. 2A). Neither the percentage of chromaffin cells exhibiting spontaneous APs (80.5%, $n = 33/41$ cells and 81.6%, $n = 31/38$ cells for WKY rats and SHRs, respectively, $p > 0.9999$, Fisher's exact test) nor the discharge frequency (0.69 ± 1.07 Hz, $n = 32$ cells for WKY rats and 0.45 ± 0.63 Hz, $n = 31$ cells for SHRs, $p = 0.2964$, unpaired t test, Fig. 2B, left graph) significantly differed between SHRs and WKY rats. Likewise, the frequency distribution was not different between SHRs and WKY rats, $p > 0.9999$, Fisher's exact test, Fig. 2B, right histogram).

The loose patch configuration allowing for long-lasting recordings, we next analyzed the spiking pattern of WKY and SHR chromaffin cells. Do they exhibit a regular and/or a bursting pattern, as previously identified in mouse chromaffin cells [30]? To discriminate between the two firing patterns, the regularity of the firing discharge was investigated by calculating the coefficient of variation (CV) of inter-spike interval (ISI) distribution. The analysis of the discharge pattern (150–200 s recording) was performed on 24 WKY and 26 SHR chromaffin cells (8 and 7 rats, respectively), and showed that WKY and SHR cells both fire regularly or in bursts (Fig. 3A and B and Figure S2). As expected and consistent with previous data in mouse chromaffin cells [30], a regular firing mode is associated with a CV < 1 and a

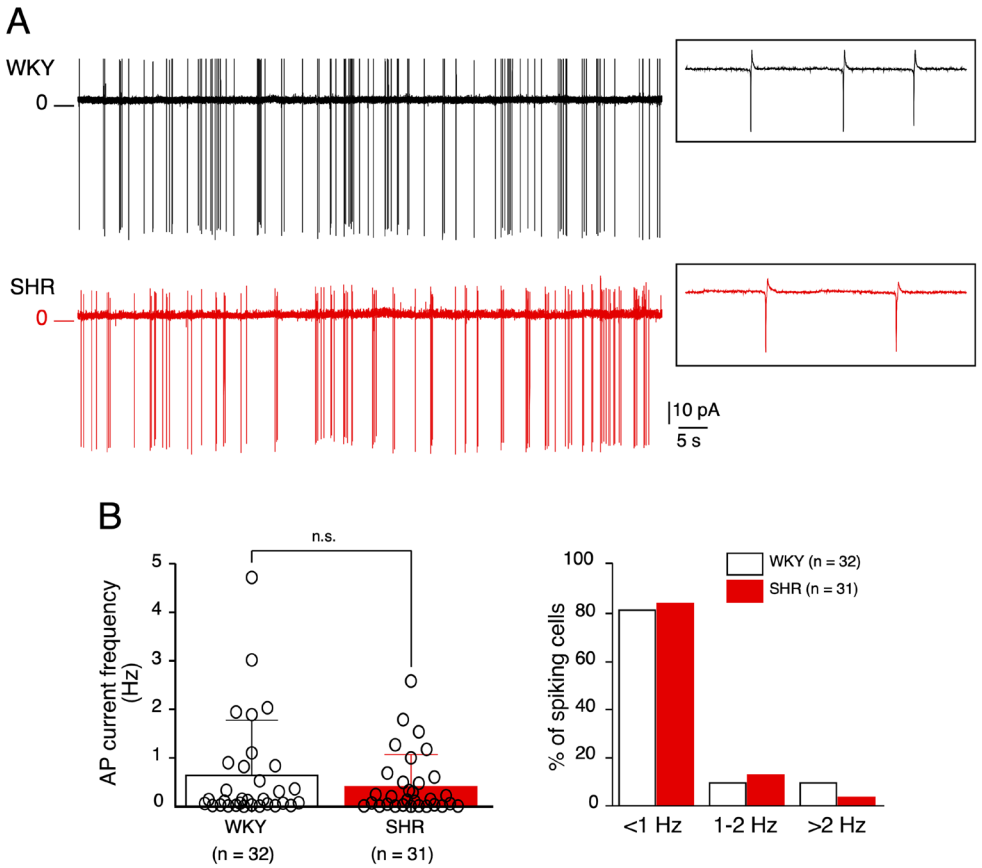

Fig. 2 Spontaneous electrical firing monitored in chromaffin cells in adrenal acute slices of WKY rats and SHRs. Action potential (AP) currents were recorded in the voltage-clamp mode (0 mV, 100 s duration) of the loose cell-attached configuration. **(A)** Representative chart recordings of a WKY (upper trace) cells and a SHR (lower trace) cell. **(B)** Analysis of the AP current frequency (only cells exhibiting APs were analyzed). Neither the mean frequency nor the distribution (ranging from < 1 to > 2 Hz) differed between WKY rats and SHRs. Values and error bars represent mean and SD (32 WKY cells and 31 SHR cells, left graph: unpaired t test, $p > 0.05$; right histogram: Fisher's exact test, $p > 0.05$)

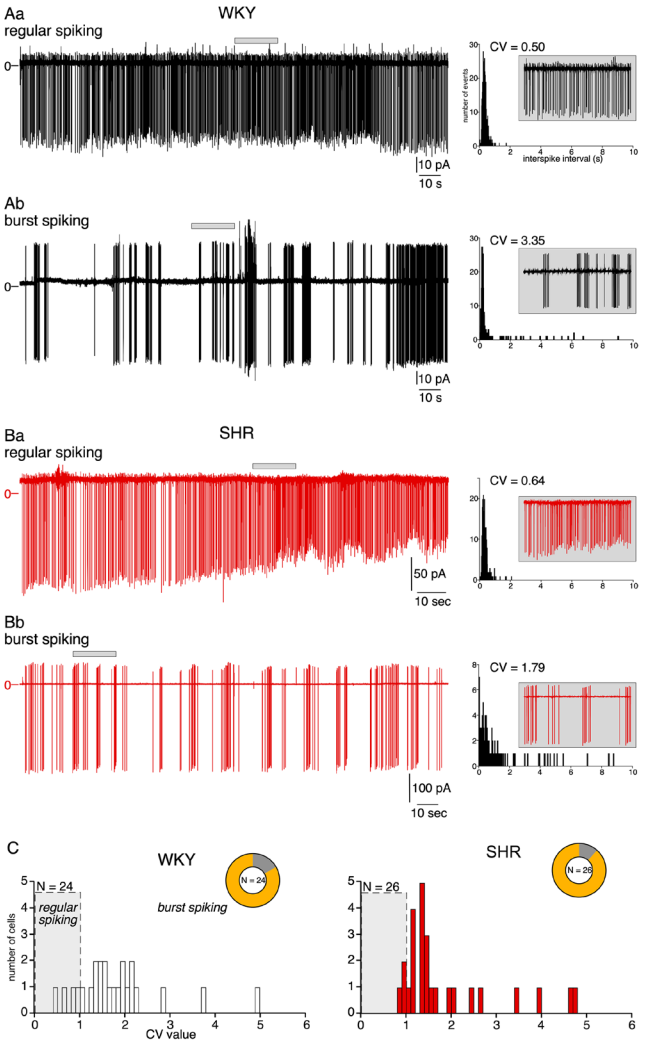

Fig. 3 Presence of two distinct firing patterns in chromaffin cells of WKY rats and SHRs. Cells were recorded in the loose cell-attached configuration and voltage-clamped at 0 mV. **(A)** Spontaneous AP currents recorded in two individual cells of WKY rats. One cell exhibits a regular spiking (**Aa**, coefficient of variation CV = 0.5), while the second cell displays a bursting firing pattern (**Ab**, CV = 3.35). The histograms on the right illustrate the distribution of the inter-spike intervals (100 ms bin), from which the coefficients of variation (CV) were calculated, as described in [30]. **(B)** Spontaneous AP currents recorded in two individual cells of SHRs. One cell exhibits a regular spiking (**Ba**, coefficient of variation CV = 0.64), while the second cell displays a bursting firing pattern (**Bb**, CV = 1.79). Insets in A and B: expanded time scale illustrating a 20-s spiking period. **(C)** Histograms illustrating the distribution of the mean CV values calculated in 24 WKY cells and 26 SHR cells (0.1 CV unit bin) (Fisher's exact test, $p > 0.05$)

bursting mode with a CV > 1. No overt difference in the percentage of cells displaying a regular or a bursting firing was observed between SHRs and WKY rats (3 regular and 23 bursting cells ($n = 26$) for SHR and 4 regular and 20 bursting cells ($n = 24$) for WKY, respectively, $p = 0.6971$, Fisher's exact test, Fig. 3C). To determine whether the two firing patterns account for two distinct chromaffin cell populations or can occur in the same cell, the spontaneous electrical activity of individual chromaffin cells was recorded for a longer period of time (5–15 min, loose-patch configuration). Interestingly, both in WKY rats and SHRs, the firing discharge can alternate between the two modes within the same cell, switching from a regular to a bursting mode and vice-versa (Figure S3), indicating that these spiking patterns do not reflect two different chromaffin cell populations.

To further investigate chromaffin cell excitability, depolarizing steps were evoked using the whole-cell configuration in cells current-clamped at their resting membrane potential (between −60 and −70 mV) (Fig. 4A). APs were elicited during 500 ms from a rheobase of 14.8 ± 9.4 pA ($n = 26$ cells) for WKY rats and 11.5 ± 5.7 pA ($n = 24$ cells) in SHRs ($p = 0.1479$, unpaired t test). When plotting the AP frequency as a function of the injected current intensity, no significant difference was found between SHRs and WKY rats in response to small depolarizing currents (≤ 40 pA). Conversely, when injecting large current amplitudes (> 40 pA), the AP accommodation increased in SHRs, leading to a significant reduction in firing frequency at 60 pA (23.0 ± 5.0 Hz, $n = 12$ for SHRs *versus* 28.5 ± 4.4 Hz, $n = 13$ for WKY rats, $p = 0.0087$, Mann-Whitney test, Fig. 4B). These AP frequency values are likely close to the maximum AP frequency that a rat chromaffin cells can withstand (see also Figure S7A for data in a computational chromaffin cell model). The reduction in spiking frequency in SHRs was associated with a gradual drop of the AP peak (-34% between the second AP and the last AP in SHRs *versus* −25% in WKY rats) and a spike widening (+20% between the second AP and the last AP in SHRs *versus* +16% in WKY rats, $p < 0.001$, unpaired t test, Fig. 4C). This observation is particularly relevant in that robust depolarizations may simulate the elevated peripheral sympathetic tone associated with elevated blood pressure. For spontaneous APs recorded in current-clamp mode without current injection, as for evoked APs, the duration was higher (+63% half-width) and the amplitude was lower in SHRs compared to WKY rats (-11%, Fig. 4D, mean of 30–50 successive APs). The overall features of evoked and spontaneous APs in SHRs and WKY rats are summarized in Table S2. Collectively, these results indicate that in response to sustained electrical stimulation with high-amplitude currents, chromaffin cells of SHRs are less excitable than those of WKY rats.

Does decreased cell excitability have functional relevance under conditions of physiological stress, a situation associated with an increase in splanchnic nerve firing discharge and change in the nature of the neurotransmitters released at the adrenomedullary synapses [21]? To address this issue, we studied the electrical behaviour of SHR and WKY chromaffin cells in response to the pituitary adenylyl cyclase-activating polypeptide (PACAP), a major

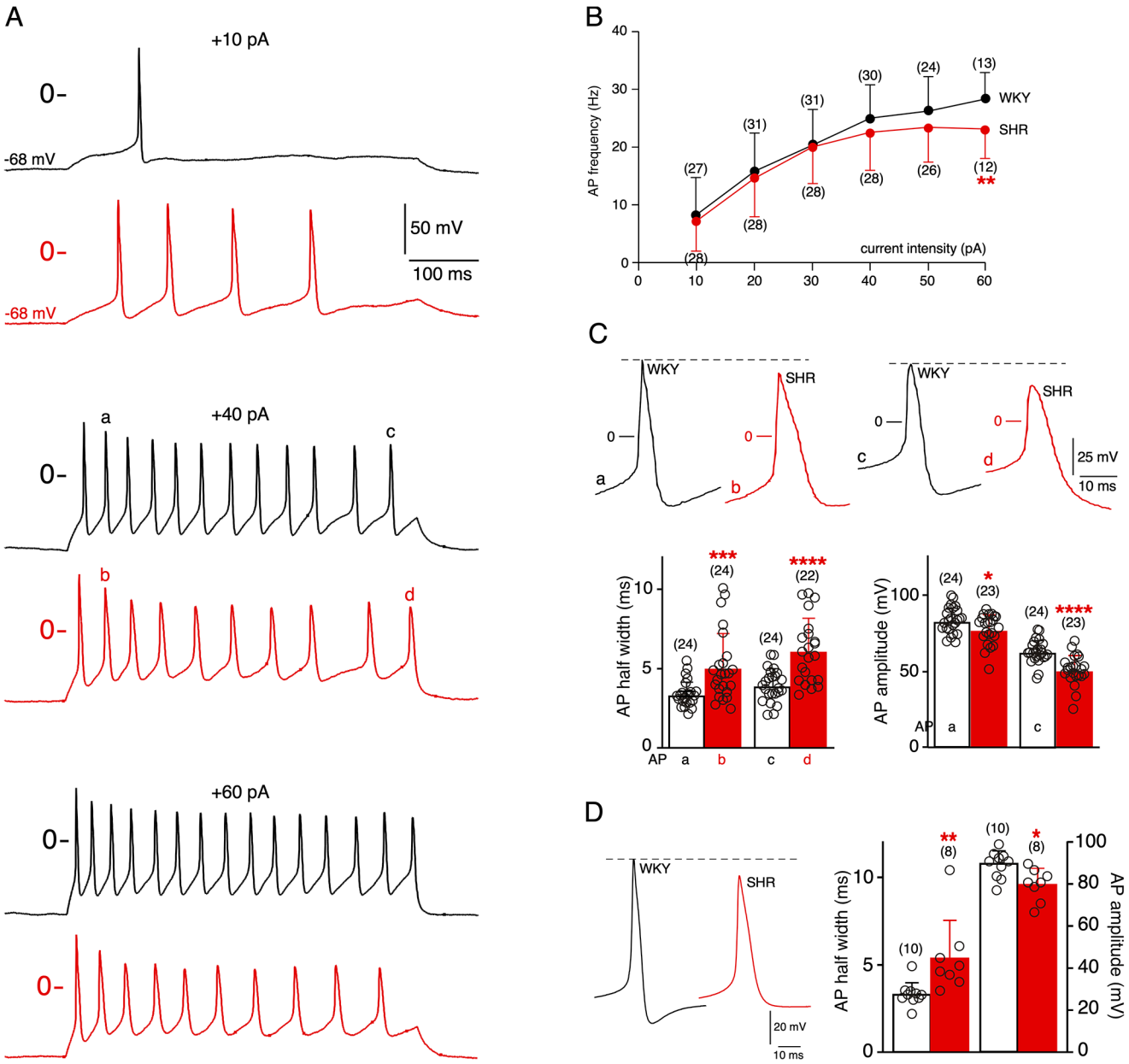

Fig. 4 Decreased chromaffin cell excitability in response to robust depolarizations and AP waveform changes in SHRs. **(A)** Illustrative chart recordings of evoked electrical activities in current-clamped WKY (black traces) and SHR (red traces) cells, in response to depolarizing steps (500 ms duration, + 10, +40 and + 60 pA injected currents as upper, middle and bottom traces, respectively). Note that the depolarization induced by a current injection of + 10 pA triggered more APs in SHR than in WKY rats (upper charts). **(B)** Analysis of the AP frequency in response to serial increasing depolarizations (the number of recorded cells for each stimulus intensity is indicated in parentheses). Robust depolarizing steps (I_{inj} ≥40 pA) elicited less APs in SHRs than in WKY rats. At I_{inj} = 60 pA, the number of APs elicited in SHRs is significantly lower than that elicited in WKY rats (values and error bars represent mean and SD, Mann-Whitney test, **, $p < 0.01$). **(C)** Single AP waveforms derived from the second (a and b traces for WKY and SHR, respectively) and the last (c and d traces for WKY and SHR, respectively) evoked APs in response to a + 40 pA, 500 ms duration depolarizing step. Analysis of AP half-width and amplitude changes shows an increased half-width and a decreased amplitude in SHRs. Values and error bars represent mean and SD (24 WKY cells and 22–24 SHR cells, unpaired t test, *, $p < 0.05$, ***, $p < 0.001$ and ****, $p < 0.0001$). **(D)** Similar analysis performed for spontaneous APs (mean of 30–50 APs/cell) recorded in WKY and SHR chromaffin cells (10 and 8 cells, respectively) current-clamped at their resting membrane potential. AP half width and amplitude are also significantly modified in SHRs (increased and decreased, respectively). Values and error bars represent mean and SD (Mann-Whitney test, *, $p < 0.05$ and **, $p < 0.01$)

neurotransmitter for stress transduction at the splanchnic nerve-chromaffin cell synapse, as reported in mice [41, 42]. Cells were recorded in the loose-patch cell-attached configuration and stimulated with 0.1 to 10 µM PACAP (Fig. 5). Representative chart recordings in response to 10 µM PACAP are plotted in Fig. 5A. AP currents were monitored before and after PACAP stimulation and the results after PACAP are presented as a percentage relative to the firing frequency observed before PACAP (Fig. 5B). At low PACAP concentration (0.1 µM), the AP current frequency did not significantly change compared to control condition without PACAP (in WKY rats: +12.7 ± 65.7%, $n = 6$ cells, Wilcoxon matched-pairs signed-rank test, $p = 0.8125$; in SHRs: +5.7 ± 6.8%, $n = 4$ cells, Wilcoxon matched-pairs signed-rank test, $p = 0.2500$). PACAP, at 1 µM, increased the frequency of AP currents in WKY chromaffin cells, but not in SHRs (in WKY rats: +208.3 ± 234.4%, $n = 7$ cells, Wilcoxon matched-pairs signed-rank test, $p = 0.0158$; in SHRs: +30.6 ± 35.4%, $n = 6$ cells, Wilcoxon matched-pairs signed-rank test, $p = 0.0938$). At higher PACAP concentration (10 µM), AP current frequency in SHRs is even significantly decreased when compared to that observed before PACAP application (in SHRs: -40.7 ± 24.4%, $n = 9$ cells, Wilcoxon matched-pairs signed-rank test, $p = 0.0039$; in WKY rats: +93.7 ± 164.8%, $n = 7$ cells, Wilcoxon matched-pairs signed-rank test, $p = 0.2969$). When compared to

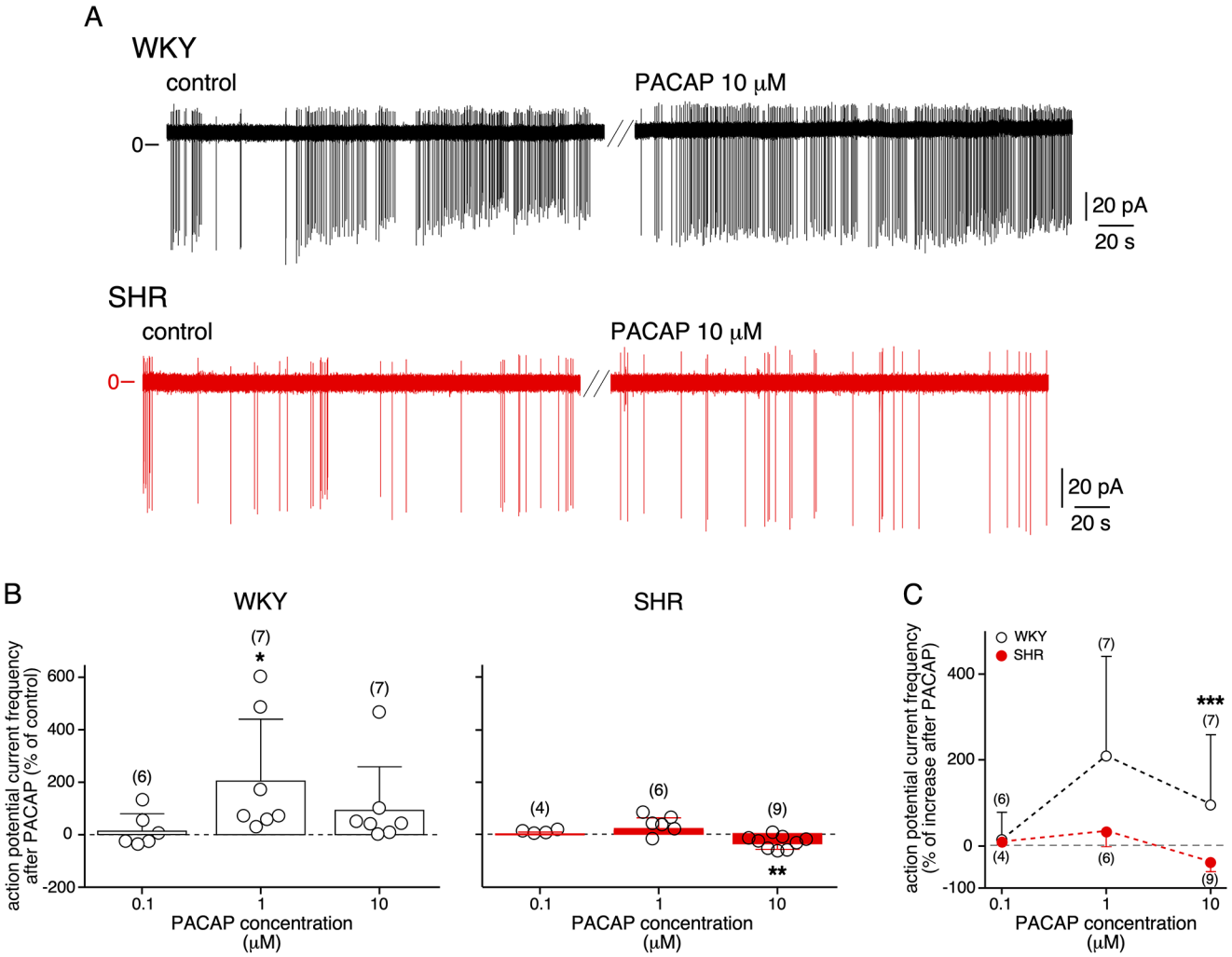

Fig. 5 Physiological consequence of reduced excitability in SHRs: lack of electrical response to PACAP. Chromaffin cells in acute adrenal slices were recorded in the loose-patch cell-attached configuration (clamped at 0 mV) and stimulated with 0.1 to 10 µM PACAP-38. **(A)** Representative chart recordings of AP currents in a WKY and SHR chromaffin cell exposed to 10 µM PACAP. **(B)** Pooled data of electrical responses to various PACAP concentration applications, illustrating the lack of response to PACAP in SHRs (right graph) compared to the increase in frequency of AP currents in WKY rats (left graph). The data are presented as a percentage relative to the firing frequency observed under control conditions (without PACAP). Note the decreased frequency in hypertensive animals upon a challenge with a high PACAP concentration (10 µM). Values and error bars represent mean and SD (Wilcoxon matched-pairs signed-rank test, *, $p < 0.05$). **(C)** Plot summarizing the effects of PACAP and the difference between SHRs and WKY rats, in particular at high PACAP concentration. Values and error bars represent mean and SD (Mann-Whitney test, ***, $p < 0.001$)

WKY cells, SHR chromaffin cells challenged with 10 µM PACAP appeared much less likely to trigger APs (Fig. 5C, Mann-Whitney test, $p=0.0003$). This result corroborates the decrease in excitability reported in Fig. 4. To investigate whether the change in cell excitability reflects changes in the firing (regular *versus* bursting) pattern, we analyzed the coefficient of variation, before and after PACAP exposure (0.1 to 10 µM, Figure S4). Although there is a downward trend, no significant differences were observed in both SHRs and WKY rats (2.22 ± 1.20 before PACAP and 1.89 ± 0.91 after PACAP, $n=12$ cells for WKY rats, $p=0.2661$, Wilcoxon matched-pairs signed-rank test and 2.25 ± 1.26 before PACAP and 1.62 ± 0.50 after PACAP, $n=10$ cells, $p=0.1934$, Wilcoxon matched-pairs signed-rank test, Figure S4A). In response to PACAP, the CV variance decreased more markedly in hypertensive than in normotensive animals, suggesting that PACAP acts by homogenizing the firing pattern of SHR chromaffin cells (Figure S4B). This is consistent with the lack of correlation observed in SHRs, between CV after and before PACAP, in contrast to WKY rats ($\rho=0.713$ in WKY rats, $p=0.0012$, $n=12$ cells, Spearman's rank correlation coefficient *versus* $\rho=0.038$ in SHRs, $p=0.916$, $n=10$ cells, Spearman's rank correlation coefficient, Figures S4Ca and S4Cb). Altogether, these data obtained in response to PACAP, a main neurotransmitter operating at the stressed splanchnic nerve-chromaffin cell synapse, open up a new avenue of investigation. From a physiological point of view, the reduced ability of chromaffin cells to be stimulated by PACAP suggests an alteration of the stress response in SHRs. This may occur at the level of catecholamine secretion, although it has not yet been established that PACAP triggers CA secretion in rat chromaffin cells, as shown in mice [41, 43].

AP waveform critically relies on the nature and the relative proportion of voltage-gated ion channels. To identify the molecular determinants that could underlie the changes in AP shape, we investigated the expression of transcripts encoding voltage-dependent ion channels by quantitative PCR (Fig. 6). We first investigated the expression level of mRNA encoding the α (Fig. 6) and auxiliary β subunits (Figure S6) of the voltage-gated sodium (Na_V1) channel family. As previously reported in mouse [44], *Scn3a* gene (encoding $Na_V1.3$) is the main Na_V channel gene expressed in the adrenal medulla of both normotensive and hypertensive rats (Fig. 6A and C), with a significant upregulation in SHRs at the transcript level (1.4-fold increase, $p=0.0260$, Mann-Whitney test, Fig. 6B), which was not observed at the protein level (Figure S5). Regarding the other Na_V1 isoforms, it is noteworthy that the expression level of *Scn9a* mRNA (encoding $Na_V1.7$) displayed a 11.5-fold increase in SHRs ($p=0.0049$, Mann-Whitney test, Fig. 6B), accompanied by a 1.3-fold increase at the protein level ($p=0.0411$, Mann-Whitney test, Figure S5). $Na_V1.1$, $Na_V1.4$ and $Na_V1.5$ transcripts (*Scn1a*, *Scn4a* and *Scn5a* genes, respectively) were not detected. Regarding Na_V1 channel β subunits, *Scn1b* ($Na_V\beta1$ subunit), *Scn2b* ($Na_V\beta2$ subunit) and *Scn3b* ($Na_V\beta3$ subunit) genes were amplified, but not *Scn4b*. A significant increase was observed for *Scn2b* (2.5-fold difference, $p=0.0022$, Mann-Whitney test, Figure S6). With respect to Ca^{2+} channels, we examined both high threshold-activated Ca_V1 (L-type) and Ca_V2 (N-, P/Q- and R-type) channels, highly expressed in chromaffin cells and low threshold-activated Ca_V3 (T-type), whose expression undergoes robust remodeling in response to stressful situations [45, 46]. *Cacna1d* (encoding $Ca_V1.3$) and *Cacna1b* (encoding $Ca_V2.2$) genes are the principal transcripts expressed in WKY rats and SHRs, with respectively a 2-fold and a 1.5-fold increase in hypertensive animals ($p=0.0022$ for *Cacna1d* and $p=0.041$ for *Cacna1b*, Mann-Whitney tests, Fig. 6A and B). The highest expression difference was found for $Ca_V2.1$ channels (*Cacna1a gene*, 2.7-fold difference in SHRs, $p=0.0022$, Mann-Whitney test). Transcripts encoding $Ca_V1.2$ (*Cacna1c*), $Ca_V2.3$ (*Cacna1e*), $Ca_V3.2$ (*Cacna1h*) and $Ca_V3.3$ channels (*Cacna1i*) were weakly expressed and their expression level did not change between normotensive and hypertensive rats. *Cacna1g* mRNA (encoding $Ca_V3.1$) was not detected. Concerning K^+ channel genes, we focused on Ca^{2+}-activated channels expressed in chromaffin cells [47], namely the large (BK) KCa1.1 (*Kcnma1* gene), the intermediate (IK) KCa3.1 (*Kcnn4*) and the small (SK) KCa2 conductance channels (*Kcnn1-3*). Still, the overall collection of channels expressed (with a prevalent expression for KCa1.1 and KCa2.3) does not qualitatively differ between WKY rats and SHRs (Fig. 6A). Quantitatively, the expression level of all transcripts, except *Kcnn2*, was significantly enhanced in SHRs (1.9-fold difference for KCa1.1, 1.6-fold difference for KCa2.1, 1.5-fold difference for KCa2.3 and 1.8-fold difference for KCa3.1). KCa4.1 (*Kcnt1*) and KCa4.2 (*Kcnt2*) mRNA were not detected. Altogether, these results show that (i) the overall repertoire of voltage-gated ion channels expressed in WKY and SHR chromaffin cells is qualitatively similar (at the transcript level), except for the Na_V1 channel family for which $Na_V1.7$ (*Scn9a*) channels become the second most expressed isoform in SHRs after $Na_V1.3$ channels and (ii) the expression ratio in SHRs for a given channel undergoes remodeling as compared to WKY rats (Fig. 6C).

Are those expression differences in voltage-gated ion channels relevant for cell electrical firing and can they account for the reduced cell excitability observed in SHRs in response to sustained depolarizations? To address this issue, the experimentally observed differences in the expression of Na^+, Ca^{2+} and Ca^{2+}-dependent K^+ channels were evaluated in a computational model of

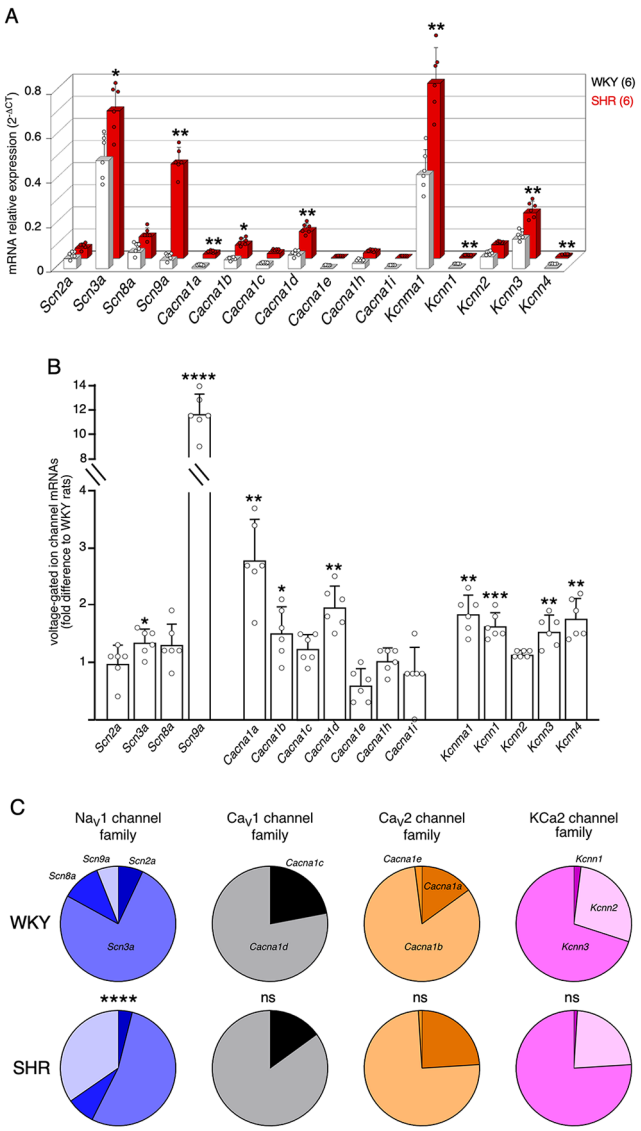

Fig. 6 Remodeling of transcripts encoding voltage-gated ion channels in SHRs. Changes in mRNA expression levels were assessed by real-time RT-PCR in macrodissected adrenal medullary tissues from 6 WKY rats and 6 SHRs. **(A)** 3D-bar graphs illustrating the relative expression levels in Na_V, Ca_V and KCa channel genes. Values and error bars represent mean and SD (Mann-Whitney test, *, $p<0.05$ and **, $p<0.01$). **(B)** Fold differences in SHRs, as compared to WKY rats. The highest fold-difference refers to *Scn9a* (encoding $Na_V1.7$, 11.7-fold increase) for the Na_V family, *Cacna4a* (encoding $Ca_V2.1$, >2.8-fold increase) for the Ca_V gene family and *Kcnma1* (encoding KCa1.1, 1.9-fold increase) for the KCa gene family. Fold difference values were determined according to Livak's method [37]. The Shapiro-Wilk test was used to analyze the normality of data distribution, and parametric or non-parametric unpaired tests were used when appropriate. Values and error bars represent mean and SD (Mann-Whitney test, *, $p<0.05$, **, $p<0.01$, ***, $p<0.001$ and ****, $p<0.0001$). **(C)** Distribution of the channel isoforms in WKY rats and SHRs showing that the same voltage-gated channel families are present in the two strains, but with different expression ratios. Note the significant difference for transcripts encoding Na_V1 channel family, associated with a decrease for *Scn3a* and an increase for *Scn9a* in SHRs. Percentages were compared using a contingency table and the chi-square test (****, $p<0.0001$). ns, not statistically different

the rat chromaffin cell electrical activity [34] (Fig. 7). The WKY and SHR models were implemented by the respective experimental values of resting membrane potential and membrane capacitance (see Table S1). For the WKY model, the values for G_{Na}, G_{Ca}, G_{BK} and G_{SK} were directly extracted from Warashina's model. To build the SHR model, (i) we assumed that the transcriptional differences equally mirror protein expression level and (ii) because the electrical firing pattern results from the concomitant contribution of Na_V, Ca_V and Ca^{2+}-dependent K^+ channels, we chose to change the conductance values globally, rather than individually (see data in Figure S7 for individual changes in G_{Na}, G_{Ca} or $G_{SK/BK}$). The conductance values implemented into the model were extrapolated from the differences in the expression level of the most abundant transcript for Na_V, Ca_V and Ca^{2+}-dependent K^+ channels, that are $Na_V1.3$ (1.4-fold), $Ca_V1.3$ (2-fold) and KCa1.1/KCa2.3 (1.7-fold) (Fig. 6B). Depolarizing voltage steps (500 ms duration) of gradually increased stimulation intensities (10 to 35 µA/cm^2) were injected into the WKY and SHR models. Representative APs evoked for three stimulation intensities are illustrated in Fig. 7A. For low intensity stimulation ($\leq$23 µA/cm^2), the SHR model generates more APs than the WKY model, as observed experimentally (Fig. 4A, upper charts). Consistent with the data obtained in the loose-patch configuration, high stimulation intensities (>23 µA/cm^2) triggered less APs in the SHR model. Pooled data indicate that AP frequency is maximal for stimulations >30 µA/cm^2 and saturates at 24–26 Hz for WKY and 12 Hz for SHR models (Fig. 7B, red trace). Collectively, the simultaneous modification of G_{Na}/G_{Ca}/$G_{SK/BK}$ (x1.4/x2/x1.7) leads to a pronounced and significant reduction in AP frequency (two-way ANOVA followed by a Bonferroni's post-hoc test, $p<0.001$). Since *Scn9a* encoding $Na_V1.7$ channel was highly expressed in SHRs (Fig. 6) and although the most abundant transcript for Na_V channels in these animals remains that encoding $Na_V1.3$, we also added a $Na_V1.7$ component to the computational model, resulting in the following parameters: $Na_V1.3$/$Na_V1.7$ (3-fold), $Ca_V1.3$ (2-fold) and KCa1.1/KCa2.3 (1.7-fold) (Fig. 7B, purple trace). Increasing G_{Na} (3-fold change) in the SHR model also results in a pronounced and significant reduction in AP frequency compared to the WKY model (two-way ANOVA followed by a Bonferroni's post-hoc test, $p<0.01$). As such, and despite the fact that the SHR model was compiled on the basis of transcriptional differences, our data suggest that a coordinate increase in Na_V, Ca_V and Ca^{2+}-activated K^+ channels can account for the reduced excitability of SHR chromaffin cells, that occurs in response to robust depolarizations.

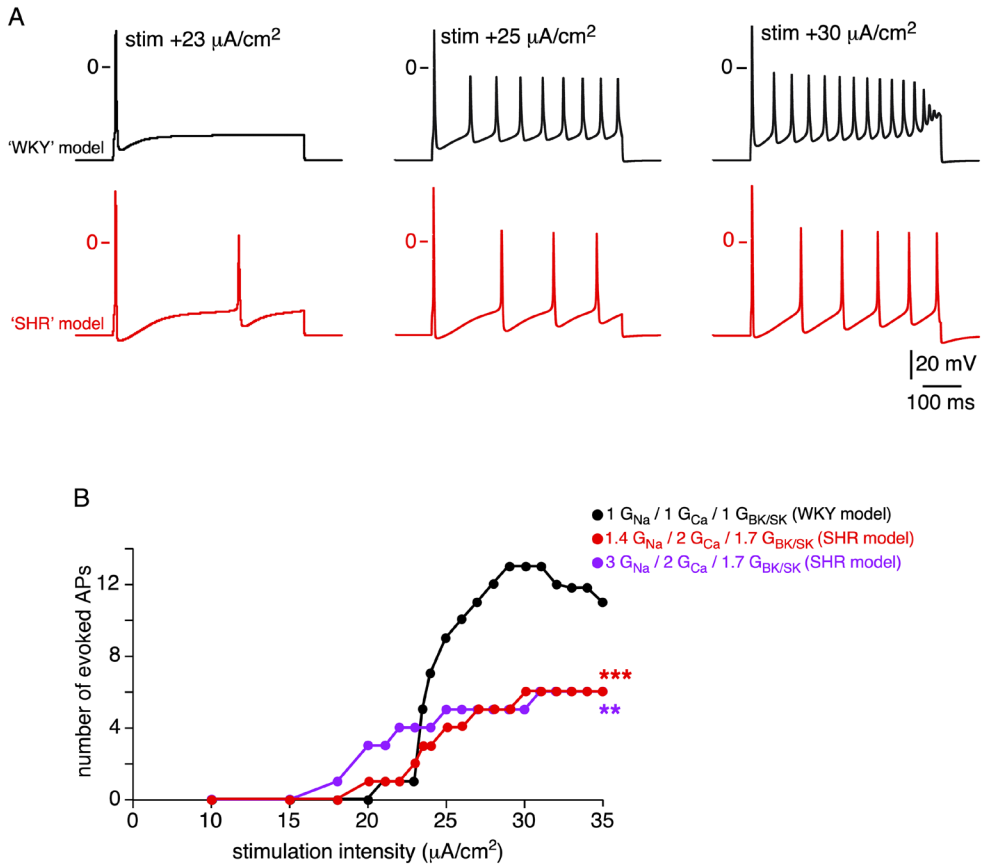

Fig. 7 Computational simulation of the electrical firing of WKY and SHR chromaffin cells: reduced excitability in SHR model in response to sustained depolarizations. WKY and SHR models were built from the rat chromaffin cell computational simulation developed by Warashina and Ogura [34]. The SHR condition was simulated by adding a multiplier (derived from the transcriptional changes) to Na^+, Ca^{2+} and Ca^{2+}-dependent K^+ conductances, as such the SHR model = 1.4 G_{Na}, 2 G_{Ca} and 1.7 $G_{SK/BK}$ WKY model. The stimulation intensity was gradually increased from 10 to 35 µA/cm^2 (500 ms depolarizing steps). **(A)** Representative APs extracted from WKY (black traces) and SHR (red traces) models plotted for three stimulation intensities. **(B)** Pooled data showing pronounced and statistically significant reduction in AP frequency in two SHR models (1.4 G_{Na}, 2 G_{Ca} and 1.7 $G_{SK/BK}$, red trace and 3 G_{Na}, 2 G_{Ca} and 1.7 $G_{SK/BK}$, purple trace), in response to robust depolarizations (> 23 µA/cm^2, two-way ANOVA followed by a Bonferroni's post-hoc test, **, $p < 0.01$ and ***, $p < 0.001$)

Changes in cholinergic synaptic transmission in hypertensive rats

Besides chromaffin cell excitability, cholinergic synaptic transmission at the splanchnic nerve-chromaffin cell junction is a key element of the stimulus-secretion coupling in the adrenal medulla. We therefore monitored the behaviour of cholinergic synapses by recording spontaneous excitatory postsynaptic currents (sEPSCs) in chromaffin cells voltage-clamped at -80 mV, as described [31]. Consistent with previous studies [32, 48, 49] and reflecting the large number of nerve fibers cut during the slicing procedure [33, 50], few chromaffin cells exhibited sEPSCs in standard 2.5 mM K^+-containing saline (36.7%, $n = 18/49$ in WKY rats *versus* 23.1%, $n = 12/52$ in SHRs, $p = 0.1909$, Fisher's exact test). Figure 8A illustrates representative charts of sEPSCs recorded in WKY (upper trace) and SHR (lower trace) chromaffin cells voltage-clamped at -80 mV, in response to a 80 mM KCl puff to increase the number of synaptic events. Mean sEPSC amplitude did not significantly differ between SHRs and WKY rats (133.1 ± 76.3 pA, $n = 7$ cells in SHRs and 106.3 ± 53.7 pA, $n = 8$ cells in WKY rats, $p = 0.4634$, Mann-Whitney test). Conversely, sEPSC frequency was significantly lower in SHR chromaffin cells (2.5 ± 2.2 Hz, $n = 7$ cells in SHRs *versus* 5.3 ± 2.2 Hz, $n = 8$ cells in WKY rats, $p = 0.0093$, Mann-Whitney test). sEPSC kinetic parameters were also analyzed (Fig. 8B). No difference was observed on the activation phase (rise time of 2.04 ± 0.25 ms, $n = 8$ cells and 2.18 ± 0.30 ms, $n = 7$ cells for WKY and SHR rats, respectively, $p = 0.3357$, Mann-Whitney test). By contrast, when the decay phase was fitted by a single exponential curve [32, 51], a significant increase in the time constant was observed in SHRs (t = 15.58 ± 2.19 ms, $n = 8$ cells for WKY rats *versus* 23.82 ± 5.25 ms, $n = 7$ cells for SHRs, $p = 0.0037$,

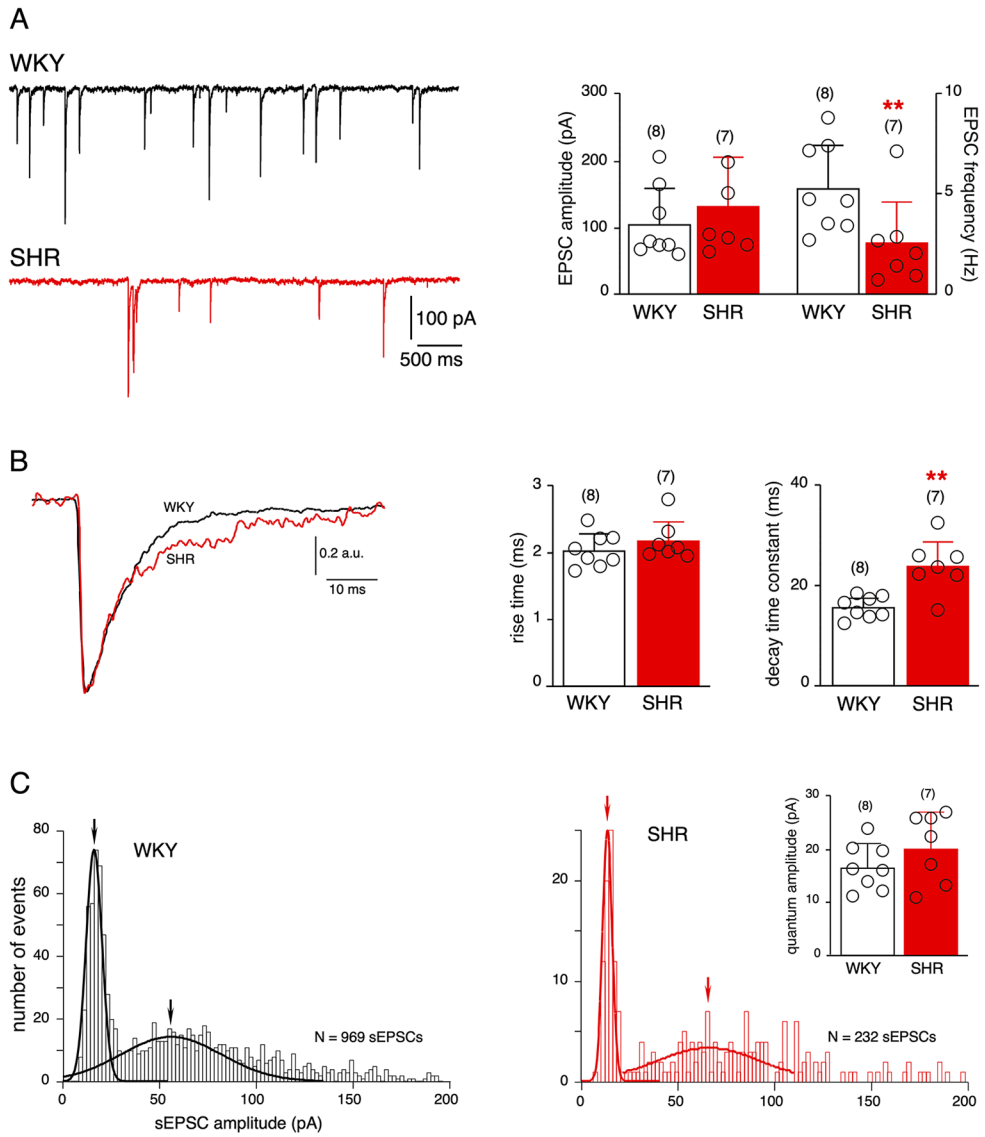

Fig. 8 Changes in the excitatory cholinergic synaptic neurotransmission between splanchnic nerve endings and chromaffin cells in SHRs. **(A)** Typical chart recordings of excitatory postsynaptic currents (EPSCs) recorded in WKY (upper trace) and SHR (lower trace) chromaffin cells voltage-clamped at -80 mV, in response to an 80 mM KCl puff. The analysis of synaptic transmission shows a significant decrease in EPSC frequency in SHRs (right graphs). No difference was observed in EPSC amplitude. Values and error bars represent mean and SD (8 WKY chromaffin cells and 7 SHR chromaffin cells, Mann-Whitney test, **, $p < 0.01$). **(B)** In regard to EPSC kinetics, superimposed normalized WKY and SHR EPSCs and associated data graphs illustrate a significant elongated EPSC decay time in SHRs. Values and error bars represent mean and SD (Mann-Whitney test, **, $p < 0.01$). **(C)** Analysis of EPSC quantal size. Histograms (2 pA bin) illustrate of the distribution of sEPSC amplitudes in a WKY (left) and a SHR (right) chromaffin cells. Quantal size was estimated from the mean value of the first Gaussian curve fitted to the amplitude distribution histogram. As summarized from the 8 WKY cells and the 7 SHR cells in which the quantal analysis was performed, the EPSC quantal size does not differ between the two strains (Mann-Whitney test, $p > 0.05$)

Mann-Whitney test). The quantal analysis of sEPSCs did not show any significant difference between SHRs and WKY rats (16.8 ± 4.4 pA, $n = 8$ cells for WKY rats and 20.5 ± 6.60 pA, $n = 7$ cells for SHRs, $p = 0.2676$, Mann-Whitney test, Fig. 8C). Collectively, these data argue for synaptic activity changes occurring both at pre- and postsynaptic sites.

Excitatory postsynaptic events at the rat splanchnic nerve terminal-chromaffin cell junction result from the co-activation of several nicotinic acetylcholine receptor (nAChR) subtypes [31, 32, 46, 51]. A change in the expression and/or composition of nAChRs could account for the change in sEPSC decay time constant observed in SHRs. To address this issue, the expression levels

of transcripts encoding α3 (*Chrna3*), α4 (*Chrna4*), α5 (*Chrna5*), α7 (*Chrna7*), β2 (*Chrnb2*) and β4 (*Chrnb4*) subunits was quantified by real-time RT-PCR (Fig. 9). The expression of genes encoding α3 and α7, two subunits dominantly engaged in the synaptic transmission, did not change between SHRs and WKY rats. By contrast, the transcripts encoding the two auxiliary α4 and α5 subunits were differently expressed, with a significant increase for α4 (5.7-fold, $p = 0.0043$, Mann-Whitney test) and decrease for α5 (0.57-fold, $p = 0.0043$, Mann-Whitney test) in SHRs. For the β subunit family, the expression of β4, the main β subunit expressed in rat chromaffin cells significantly decreased in SHRs (0.48-fold, $p = 0.0043$, Mann-Whitney test). *Chrnb2* expression remained unchanged. Taken together, these findings indicate that nAChR subunits are transcriptionally remodeled in SHRs. Assuming subsequent modifications at the protein level, this plasticity may contribute to the modifications observed in sEPSC kinetics.

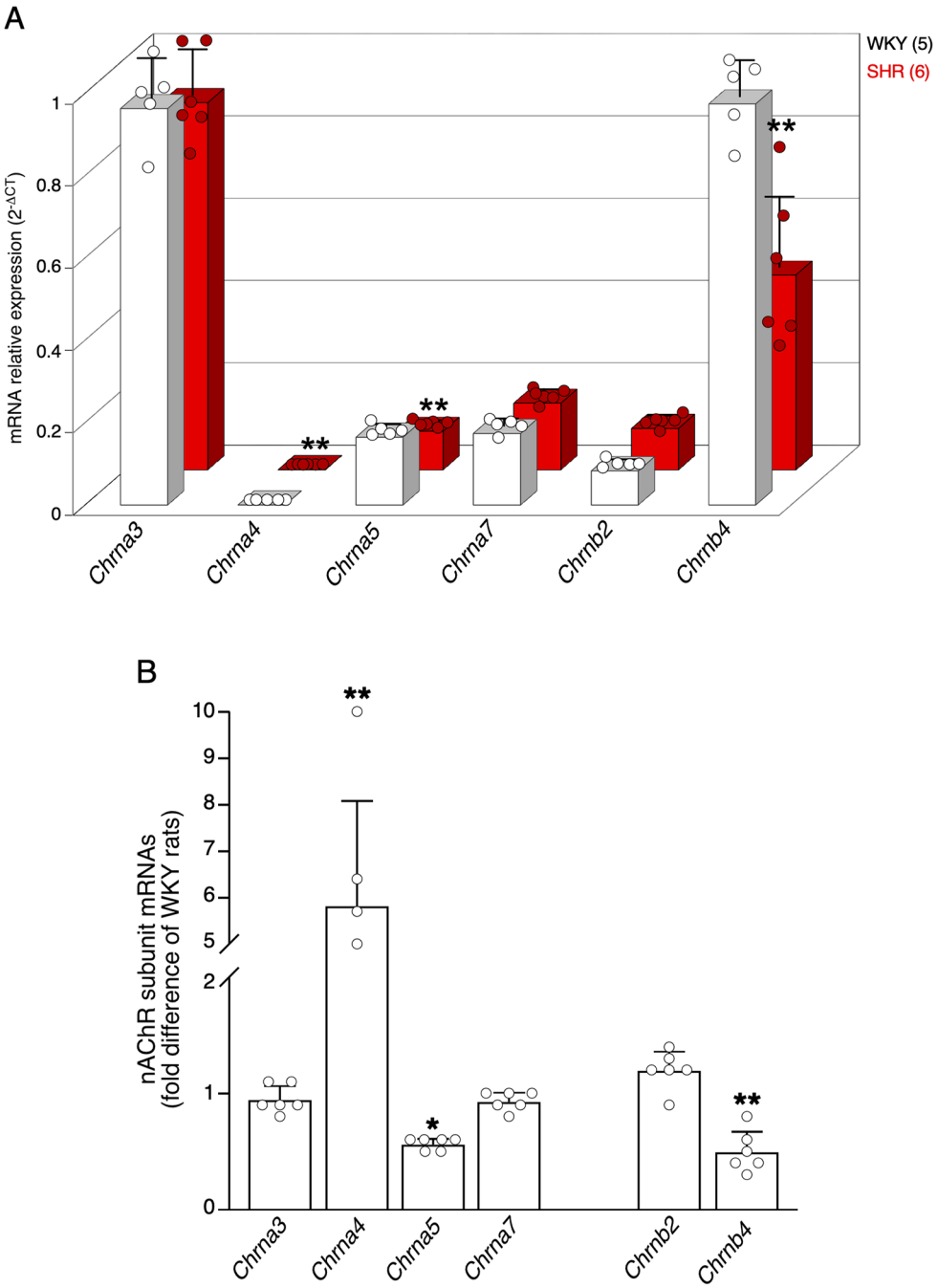

Fig. 9 Remodeling of transcripts encoding nAChR subunits in SHRs. The differences in mRNA expression level of nAChR subunits were assessed by real-time RT-PCR, in macrodissected WKY (5) and SHR (6) adrenal medullary tissues. **(A)** 3D-bar graphs illustrating the relative expression levels of four α (*Chrna3*, *Chrna4*, *Chrna5* and *Chrna7*, encoding α3, α4, α5 and α7, respectively) and two β (*Chrnb2 and Chrnb4*, encoding β2 and β4, respectively) subunit genes, in the two rat strains. Values and error bars represent mean and SD (Mann-Whitney test, **, $p < 0.01$). **(B)** Fold differences in SHRs, as compared to WKY rat. Significant differences occur for *Chrna4* (5.8-fold), *Chrna5* (0.6-fold) and *Chrnb4* (0.5-fold). Fold difference values were determined according to Livak's method [37]. The Shapiro-Wilk test was used to analyze the normality of data distribution, and parametric or non-parametric unpaired tests were used when appropriate. Values and error bars represent mean and SD (Mann-Whitney test, *, $p < 0.05$, **, $p < 0.01$)

Reduced gap junctional coupling between chromaffin cells in hypertensive rats

In the rat adrenal medullary tissue, gap junction-mediated intercellular communication between chromaffin cells is an additional pathway involved in the regulation of stimulus-secretion coupling [15, 17, 19]. Because adrenomedullary gap junctional coupling can remodel in physiological/physiopathological conditions [18, 36, 46, 48, 49, 51, 52], we compared its status between SHRs and WKY rats. To investigate whether gap junctional coupling is modified in hypertensive rats, we imaged Lucifer yellow diffusion between chromaffin cells by confocal microscopy (Fig. 10). As illustrated in panel 10 A, the percentage of Lucifer yellow-coupled cells was lower in SHRs (18%, $n = 7/38$ cells in 4 SHRs *versus* 33%, $n = 11/33$ cells in 5 WKY rats, $p = 0.1789$, contingency table and Fisher's exact test). Consistently, the expression of connexin 43 (Cx43), the main connexin expressed in the rat adrenal medullary tissue [15, 36], is significantly diminished in SHRs, both at the transcriptional (Fig. 10B, left graph, 5 WKY rats and 6 SHRs, Mann-Whitney test, $p = 0.0303$) and protein (Fig. 10C, 5 WKY rats and 4 SHRs, Mann-Whitney test, $p = 0.0159$) levels. The expression of transcripts encoding Cx36 however did not change in hypertensive rats (Fig. 10B, right graph, 5 WKY rats and 6 SHRs, Mann-Whitney test, $p = 0.5368$). These results, in addition with an increased input resistance (see Table S1) are consistent with a reduced gap junctional communication in SHRs. To go further into the mechanisms underlying the reduced expression of Cx43 in SHRs, we addressed the involvement of post-translational changes such as stability of gap junctional plaques. Anchored gap junctions at the plasma membrane bind to scaffolding proteins, such as zonula occludens-1 (ZO-1). ZO-1 has been shown to interact with various connexins, including Cx43 [53]. As shown by the densitometric analysis of immunoblots, ZO-1 expression remains unchanged in SHRs (Fig. 10D, 5 WKY rats and 5 SHRs, Mann-Whitney test, $p = 0.3095$), indicating that the impairment in Cx43 stability at the plasma membrane is unlikely the cellular mechanism whereby Cx43 expression is reduced in SHRs.

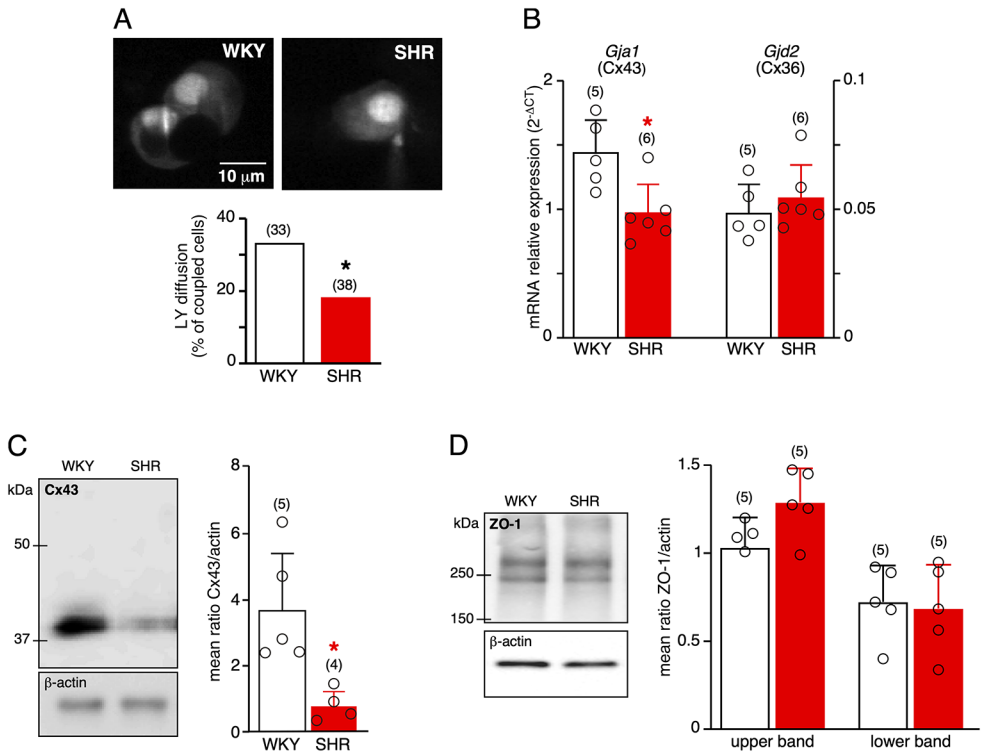

Fig. 10 Attenuated gap junction-mediated intercellular communication in SHRs. **(A)** Reduced Lucifer yellow (LY) diffusion between SHR chromaffin cells. LY was introduced into chromaffin cells using patch pipettes. Dye diffusion was imaged 15 min after patch disruption. Less than 20% of SHR chromaffin cells (38 patched cells, 4 SHRs) are dye-coupled, as compared to more than 30% in WKY cells (33 patched cells, 5 WKY rats). Percentages were compared using a contingency table and the Fisher's exact test (*, $p < 0.05$). **(B)** Decreased expression level of *Gja1* (encoding Cx43) (Mann-Whitney test, *, $p < 0.05$), but not *Gjd2* (encoding Cx36) (Mann-Whitney test, $p > 0.05$) in SHRs, assessed by real-time RT-PCR from macrodissected medullary tissues. Values and error bars represent mean and SD (5 WKY rats and 6 SHRs). **(C and D)** Western blots and associated pooled data graphs of Cx43 (**C**) and ZO-1, a Cx43-associated protein (**D**). Cx43 expression (Mann-Whitney test, *, $p < 0.05$), but not ZO-1 (Mann-Whitney test, $p > 0.05$), is significantly down-regulated in SHRs. Values and error bars represent mean and SD (5 WKY rats and 4 SHRs for Cx43 and 5 WKY rats and 5 SHRs for ZO-1)

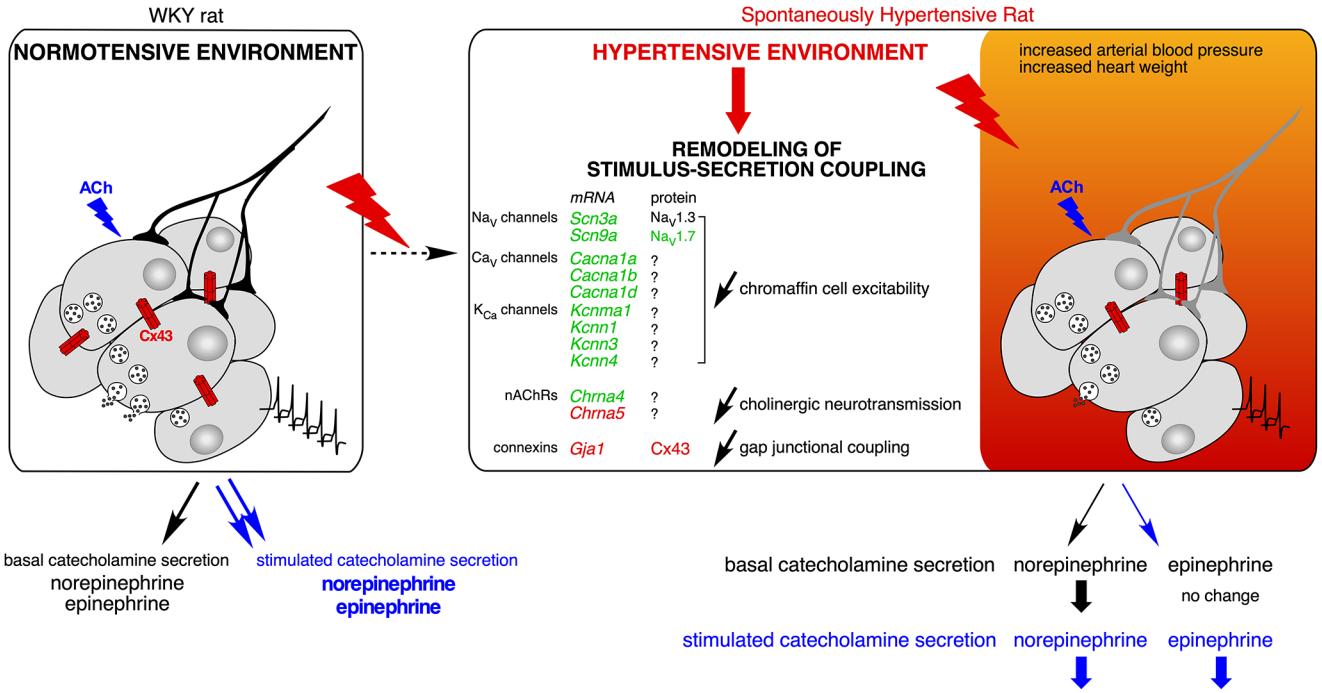

Fig. 11 Remodeling of the adrenal stimulus-secretion coupling in a chronic hypertensive environment. In response to a gradual increase in arterial blood pressure leading to hypertension, the adrenomedullary tissue adapts the secretory competence of chromaffin cells. Upon sustained agonist stimulation, the excitability of chromaffin cells, the synaptic transmission and the gap junctional communication are less efficient, resulting thus in a reduced catecholamines (epinephrine and norepinephrine) secretion. For SHR mRNAs and proteins, upward differences are shown in green, downward differences in red (?, not determined)

Discussion

This study describes the functional remodeling operated by adrenal chromaffin cells in response to chronic elevated blood pressure. All observed changes converge toward a less efficient stimulus-secretion coupling, especially in response to robust stimulations (Fig. 11). This may reflect a shielding mechanism safeguarding the hypertensive organism against the deleterious effects of excessive CA secretion.

In addition to the functional changes unveiled between normotensive and hypertensive chromaffin cells, this study also extends basic knowledge about rat chromaffin cell excitability in situ. The analysis of AP firing revealed the existence of two spiking patterns (regular and bursting), as previously reported in mice [18, 30, 54]. As in the mouse, regular and bursting discharges coexist within a same cell. Because APs generated in bursts are more efficient than AP trains fired at constant frequency to evoke CA secretion [44, 55], identifying the cellular mechanism(s) promoting the switch between the two spiking patterns would be therefore of great interest. In this context, ion channels involved in setting up the resting membrane potential appear as interesting targets to investigate [30, 56]. In addition, although we found no sharp difference in the occurrence of regular and bursting patterns between WKY rats and SHRs, further experiments are required to fully address this issue, especially in response to adrenomedullary secretagogues (neurotransmitters, neuropeptides.).

Decreased chromaffin cell excitability in response to robust depolarization/stimulation

The most functionally relevant feature of SHR chromaffin cells is their reduced AP firing in response to sustained stimulations. This likely results from a coordinated upregulation of Na^+, Ca^{2+} and Ca^{2+}_ dependent K^+ channels, as observed both experimentally with the enhanced expression level of their respective transcripts and in silico in a chromaffin cell model. At the single AP level, AP waveform in SHR chromaffin cells is modified as such the amplitude is decreased and the half-width is increased. Because the AP waveform results from the concomitant contribution of many ion channels [57], discussing each channel separately would give biased conclusions. We therefore focused the discussion on the most striking effects that is the AP waveform change and reduced ability of SHR chromaffin cells to trigger sustained firing during robust depolarizations. In chromaffin cells, as in most neurons, Na_V channels critically shape the AP waveform [58]. This is of particular importance because changes, even subtle, in spike shape can drastically affect Ca^{2+} channel recruitment and therefore ensuing Ca^{2+} transients, and finally CA secretion. Interestingly, the most remarkable

change in ion channel expression in SHRs targets $Na_V1.7$, a sodium channel involved in regulating chromaffin secretory function [59]. As reported [44], the reduced Na_V channel availability (through $Na_V1.3$ and $Na_V1.7$) switches cell firing from a repetitive AP firing mode to a bursting activity, boosting thus hormone exocytosis. At rest, Na_V channels tonically inhibit burst firing and would contribute to maintain a low basal CA secretion. In SHRs, the significant increase of $Na_V1.7$ would help retaining chromaffin cell to spontaneously fire in a tonic mode, sparing the animal from the cardiovascular challenge of large amounts of CA secretion during episodes of stress. This is consistent with our data showing that basal NE and E secretion is not enhanced in SHRs (even decreased for NE). The concomitant increased expression of $Na_V1.7$, $Ca_V1.3$ and KCa channels in SHR chromaffin cells is consonant with data reporting that (i) L-type Ca^{2+} channel activity can upregulate Na_V channels in endocrine cells [60, 61] and (ii) $Ca_V1.3$ and BK/SK channels are functionally coupled in chromaffin cells [54, 58, 62]. Long-term changes in Na_V channel expression have been also described in endocrine tissues in response to stressful situations [63]. Collectively, these findings prompt us to propose the provisional sequence of events, that is an enhancement of L-type Ca_V channels and ensuing cytosolic calcium followed by a subsequent enhancement of Na_V and KCa channels as a shielding mechanism to brake CA secretion, especially in response to prolonged or repetitive stimulations. We have focused here on voltage-gated ion channels involved in AP firing, but other ion channels, K^+/Na^+ background/leak channels operating at resting membrane potential in particular, are also qualified to modify cell excitability [30, 56, 64] and would therefore be interesting to investigate.

Weakened synaptic transmission in SHRs

In SHRs, the excitatory neurotransmission between splanchnic nerve and chromaffin cells is pre- and postsynaptically remodeled. According to the quantal theory of neurotransmitter release [65], the reduced number of sEPSCs in response to a sustained stimulation may relate to failures occurring at presynaptic components. Additionally, and supported by changes occurring postsynaptically at nAChRs, the incoming signals would be less efficiently integrated by hypertensive cells. The composition of nAChRs determines the biophysical properties and regulatory mechanisms of subsequent ACh-evoked EPSCs. In this context, our data showing a remodeling of nAChRs subunits in SHRs open up a wide field of discussion. One should keep in mind, however, that the expression of nAChRs subunits at the protein level may not parallel the remodeling observed at the transcriptional level. In chromaffin cells, the prevalent nAChR compositions encompass α3β4 and α3β2 subunits with the addition of α5 [66]. Because the β4 subunit modulates the density of α3β4 receptors at the plasma membrane [67], the decreased expression level of β4 mRNA in SHRs may reduce the membrane expression of α3β4 nAChRs and attenuate the neurotransmission at splanchnic nerve-chromaffin cell synapses. When incorporated in a nAChR, α5 subunit alters biophysical and biochemical properties of the channel [68, 69]. Of a particular interest for a neurosecretory cell is the less robust Ca^{2+} permeability of α3 nAChRs in the absence of α5 [69]. If we assume that the reduced expression level of α5 transcripts in SHRs could favor α3β2/α3β4 combinations to the detriment of α3β2α5/α3β4α5, it is likely that the resulting Ca^{2+} entry through activated nAChRs could be less robust, and could contribute to reduce hormone secretion.

In SHRs, sEPSCs exhibit a slower decay time compared to WKY rats. Although we do not have direct evidence, this difference could be explained by a change in nAChR subunit composition. Indeed, ACh-evoked currents recorded in *Xenopus* oocytes from α4-containing nAChRs decayed more slowly than those recorded from α3-containing receptors [70]. Compared to α3 subunit, little is known on the role of α4-containing nAChRs in adrenal chromaffin cells. Although α4 subunit is expressed in rat chromaffin cells [66, 71], α4-containing nAChRs contribute modestly to ACh-induced current [70]. The fact that these receptors can localize extra- or peri-synaptically [72] also argues for their non-dominant role in chromaffin cell stimulus-secretion coupling (at least under control conditions). Our data show a significant increase in the expression level of the transcript encoding α4 subunit (although it remained very poorly expressed). In parallel, the expression level of the transcripts encoding α5 and β4 subunits decreased. Assuming a faithful repercussion at protein level, we can propose that the increase in the transcript encoding α4 subunit associated with a decrease in the transcript encoding β4 subunit may favor the α4β2 combination. Interestingly, α4β2- and α3β4-containing nAChRs are differentially modulated by the α5 subunit, resulting in changes in transmitter release [73]. Given that the transcript encoding α5 has also been remodeled in SHRs, one may assume a repercussion on chromaffin cell stimulus-secretion coupling. Both α4β2 and α4β4 combinations build functional nAChRs, although the current properties differ between the two combinations [74]. The down-regulation of β4 in SHRs suggests that the prevalent combination in hypertensive rats could be α4β2 rather than α4β4. Assuming this, the current flowing through α4β2 nAChRs would

then display a lower amplitude and a faster desensitization [74]. Collectively, the transcriptional remodeling of nAChR subunit expression observed in SHRs converges towards a less efficient cholinergic coupling between nerve endings and chromaffin cells in hypertensive animals. It is of note that the stimulation of chromaffin cells with ACh not only activates synaptic nAChRs but also muscarinic AChRs (mAChRs), which are assumed to be extra-synaptically located. As recently reported in isolated chromaffin cells, CA secretion evoked by muscarine is enhanced in SHRs [75]. Accordingly, part of the CA release assayed in our study may originate from mAChRs activation. Further experiments are necessary to fully address this issue.

Reduced gap junctional coupling in SHRs

Gap junctional signaling between chromaffin cells is a part of regulatory mechanisms involved in stimulus-secretion coupling [16, 17, 19, 20]. Although we did not directly assess the junctional current, the reduced LY diffusion and the decreased Cx43 protein expression level strongly suggest an attenuated gap junctional communication in SHRs. Changes in chromaffin cell input resistance and capacitance, two parameters impacting the transmission strength and therefore the propagated signals [76], also support this statement. Given that gap junction coupling contributes to CA secretion [15, 18, 20, 36], a decreased intercellular communication could be a suitable mechanism whereby the adrenal medulla would damper its secretory process, especially in response to harmful challenges (such as repetitive stimulating episodes accompanying stressful situations). Regarding gap junctional communication, this would be particularly relevant given that (i) the expression of the two main connexins coupling rodent chromaffin cells is increased in stressed animals [18, 49, 77] and (ii) PACAP, a major neurotransmitter for stress transduction at the adrenomedullary synapse, can enhance the electrical coupling between chromaffin cells [52]. Another interesting point would be to follow over time the level of connexin expression (or the functional coupling between cells), in relation to the development of hypertension. In this context, SHRs would be a relevant animal model, as hypertension gradually develops with age [22]. In rats, connexin-mediated intercellular coupling between chromaffin cells vary with age [48, 51], but also with physiological or pathological conditions [19, 20, 36], highlighting a major contribution to adrenal stimulus-secretion coupling. Investigating which changes first, the gap junctional communication or the arterial blood pressure, would provide a further clue to the dynamic aspect of the remodeling that we observed in adult animals with chronic hypertension.

Reduced CA release in SHRs in response to sustained cholinergic stimulations

Our results argue for a decrease in the stimulus-secretion coupling efficiency in SHRs. E and NE secretion is attenuated in SHRs, especially in response to high ACh concentrations, corroborating findings obtained in isolated adrenal medulla in response to a nicotinic stimulation [78]. At rest and for lower ACh concentrations, only adrenal NE outflow is decreased, as previously reported [78]. This suggests that the hypertensive environment (circulating levels of CA and other adrenomedullary hormones/factors, adrenocortical secretions…) differentially impacts the mechanisms involved in regulating NE and E release. However, besides their difference in secretory competence, the hypertensive and normotensive medullary tissues are equally readily responsive to a cholinergic stimulus, as shown by equivalent stimulation ratios. Interestingly, they differ in the E:NE ratios in response to a cholinergic stimulus. Whereas in WKY rats, E:NE ratio increases gradually with ACh concentration (due to enhanced E release, as expected in a healthy adrenal medulla), it remains constant in SHRs, suggesting a dysregulation in the secretory process of E and/or morphometric changes of the adrenal medulla. Regarding a functional dysregulation, many targets (secretory granules, exocytosis.) can be involved and further experiments are needed to identify the impaired processes. Alternatively, the anatomy of the chromaffin tissue must also be considered. Indeed, in adult SHRs, (i) the adrenal medulla is enlarged and the dimensional ratio of NE-storing cell lobules is about twice as large as that of WKY rats [79], (ii) the NE content of SHR medulla is increased by about 2 while E content did not significantly differ between SHRs and WKY rats [80] and (iii) the number of NE-containing granules in SHR chromaffin cells is increased by 1.3 [81].

Several explanations can account for the decreased stimulus-secretion coupling efficiency in SHRs. First and supported by our electrophysiological data, SHR chromaffin cell less robustly fire upon strong depolarizations. This, in association with the remodeling of nAChR subunits, likely contributes to lessen electrical activity- and cholinergic-evoked $[Ca^{2+}]i$ rises, and subsequent CA exocytosis. Second, downstream changes may also occur, targeting for example CA biosynthesis and/or intra-adrenal content. Regarding this and partly because the animals come from different breeding farms, the literature is puzzling, that is either an increase or a decrease in activity/mRNA expression level of tyrosine hydroxylase (TH), dopamine beta-hydroxylase (DbH) and phenylethanolamine N-methyltransferase (PNMT) in adult SHRs have been described [82–87]. Similarly, the intra-adrenal CA content in adult SHRs has been reported to be either decreased, increased

or unchanged [78, 84, 87–90], making it difficult to draw any conclusions. Along the same line, the secretory granules could also be impacted. Of particular interest are the granins, major components of chromaffin granules critically involved in granulogenesis, granule cargo and exocytosis [91, 92]. By regulating circulating CA levels, granins and their derived peptides are potent modulators of blood pressure [93–95]. In adult SHRs, the increased adrenal content of chromogranin A [84, 89] is likely one of the mechanisms contributing to elevated blood pressure. Of particular interest is our finding that basal secretion of NE, but not E, is impaired in SHRs, suggesting that molecular targets/mechanisms are altered in CA biosynthesis pathway. In this context, PNMT, the enzyme that methylates NE to form E, could be one relevant target. Indeed, in SHRs, PNMT displays differences in mRNA, protein expression and enzymatic activity compared to WKY rats. The expression level of *Pnmt* transcript is up-regulated in adult SHRs [96] with conceivable repercussions on the biosynthesis of E from NE, although PNMT enzymatic activity does not appear to change [97, 98]. Interestingly and reinforcing the idea that PNMT is a major target of the hypertension in the adrenal tissue, *Pnmt* mRNA level positively correlates with systolic blood pressure [86]. At least two explanations, which are not mutually exclusive, could account for the impairment of NE secretion, (i) a decrease in NE adrenal content [87, 99] and/or (ii) an impairment of the exocytosis machinery targeting NE-containing secretory granules, as observed for the release of NE from SHR sympathetic nerves [100]. This latter hypothesis is congruent with the studies reporting an increase in NE content in the adrenal glands. Alternatively, a different turnover of NE and E would also be a valid explanation. So many morphofunctional parameters can be remodeled in adult SHRs in relation to NE biosynthesis and secretion that it becomes challenging, if not impossible, to depict an overview.

Physiological and/or pathological consequences of attenuated stimulus-secretion coupling in adult SHRs: a shielding mechanism of the adrenal medullary function and/or impairment of the stress response?

The question is open to debate. From a physiological point of view, our finding of a reduced stimulus-secretion coupling in the SHR adrenal medulla is functionally relevant and helps to decode how chromaffin cells behave to cope with a hypertensive environment, and more generally with a chronic hyperactivity as observed during a sustained splanchnic nerve firing activity evoked by prolonged stress episodes. The reduced release of adrenal CA would also preserve from exhaustion of the secretory process, maintaining therefore the tissue still competent for further stimulations, particularly with regard to E secretion. To avoid a prolonged increase in plasma CA concentration, the implementation of regulatory mechanisms is required. In adult SHRs, in whom arterial hypertension is established, plasma E/NE amounts do not differ from age-matched WKY rats [11, 23, 90]. This nicely parallels our data showing that basal E secretion does not differ between SHRs and WKY rats. Regarding basal NE, the decreased release we reported here could be seen as a discrepancy with the literature, but one should keep in mind that while plasma E levels reflect mainly, if not solely, the secretory activity of the adrenal medulla, circulating NE originates mostly from sympathetic nerve endings. Our data on E and NE secretion are, however, in agreement with those published by Moura and colleagues, who monitored spontaneous E and NE outflows from superfused adrenal glands [78]. In the same context, given the importance of CA in the control of hemodynamic properties (heart rate, cardiac output, blood pressure, vascular tone), the reduced NE outflow observed at rest and for lower ACh concentrations could be physiologically relevant to mitigate the deleterious consequences of a hypertensive environment. Indeed, by activating α-adrenoceptors, NE increases peripheral arterial resistance and therefore blood pressure. E by acting on both α- and β-adrenoceptors has also a hypertensive effect, but in a lesser extent compared to NE. Beyond their hemodynamic properties, plasma CA, when chronically elevated, can promote pathophysiological conditions including inflammation, metabolic disorders, and organ failures [101, 102]. In this context, any mechanism aimed at reducing plasma CA levels can be considered protective.

In the same line, we can also propose that the remodeling of the adrenal medulla in hypertensive animals could prevent excessive energy expenditure at both tissue and organism levels. CA synthesis and secretion are energy-consuming processes [103], so we speculate that weakening the competence of the adrenal medulla to release catecholamines could limit this energy cost. In addition, since elevated catecholamine secretion is known to induce an increase of energy expenditure mediated by metabolism stimulation [104], the remodeling we describe here would be beneficial to limit catecholamine secretion.

Adrenal medulla-driven adaptive mechanisms are decisive for the ability of an organism to cope with stress ([77] for a recent review) and any dysfunction or imbalance in one of these mechanisms can jeopardise its survival. One issue, not investigated here, would be to evaluate whether and how SHRs and more generally hypertensive animals adapt to stress (acute/chronic). Does the hypertensive adrenomedullary tissue undergo remodeling of chromaffin cell excitability, synaptic cholinergic/peptidergic neurotransmission and gap junctional coupling, as reported in normotensive stressed animals [18, 31, 36, 49, 77]? Does the adrenal medulla in SHRs still competent to secrete CA in response to an acute stress, as reported for acute hypoxia-induced CA

release in rats with chronic intermittent hypoxia [105]? The observation of a decrease in the surface area of NE-storing cell islets in adult SHR subjected to rotating exercise is consistent with a positive answer to this question [106]. In this context of stress-induced adrenomedullary response, PACAP, a major stress transmitter at the splanchnic nerve-chromaffin cell synapse [42], is certainly an avenue to explore in rats. Our data showing an alteration of the electrical response to PACAP together with (i) the previously reported effect of PACAP on *Pnmt* gene expression [107] and (ii) an increased expression of *Pnmt* mRNA and protein levels in SHRs [86, 96] may suggest altered (defective?) adrenergic transduction pathways/function in SHRs. From a functional point of view, the issue of whether PACAP-evoked CA secretion is impaired in SHRs (as was found here for ACh-stimulated secretion) would deserve further attention.

Limitations

In our study, we used only male rats and thus we do not know whether any of the identified mechanisms supporting the adaptive remodeling in a chronic hypertensive environment interact with sex. To use sex as a covariate would require a larger number of animals, which was not logistically and financially feasible. We chose to use males rather than females for compatibility with existing data, as the majority of published data on adrenal stimulus-secretion coupling were in male rats. Additionally, using males avoided inter-individual variation due to estrous cycle. This is particularly relevant for experiments investigating the remodeling of gap junction-mediated coupling, as Cx43 expression is hormone-sensitive.

Other limitations of our study were (i) to only use adult animals while hypertension develops gradually from young/juvenile age, occluding thus the time course of the changes. Here again, our choice was dictated by logistically and financially concerns, and (ii) to investigate the remodeling of stimulus-secretion coupling in unstressed animals. As E is the main catecholamine secreted in response to stress, it would have been relevant to carry out further experiments in stressed animals, in which we know that the stimulus-secretion coupling in chromaffin cells remodels. This would have helped to compare E is secreted under basal (i.e. unstressed animals) and stimulated conditions (stressed animals), and perhaps to highlight different mechanisms between these two situations.

A final limitation of our study deals with PACAP, with the unresolved questions of whether or not PACAP triggers CA secretion in rat chromaffin cells, as reported in mouse [41, 43] and if so, whether PACAP-induced CA release is altered in SHRs. Due to the discontinuation of SHRs production in France by our supplier Janvier Labs, we have been unable to complete our study and provide data on PACAP-induced CA secretion.

Conclusion

The adrenal stimulus-secretion coupling is a dynamic process, continuously remodeled according to physiological or pathophysiological conditions [46, 108]. Whereas acute CA needs (as required during stressful situations) are associated with an increased stimulus-secretion coupling efficiency [18, 36, 49], a long-lasting impregnation of the adrenal medullary tissue with high circulating CA levels (as seen during the development of hypertension, for example) would correlate with reduced competence of stimulus-secretion coupling. Other chronic pathological conditions can threaten the body's homeostasis and activate the adrenal glands. Chronic intermittent hypoxia (IH), in this respect, is an interesting example, in which the adrenal glands play a major role [109]. Interestingly, chronic IH stimulates CA efflux from the adrenal medulla, which contributes at least in part to increased blood pressure. More remarkably, in a chronic IH environment, CA (E and NE) secretion evoked by high nicotine concentration is reduced [105]. It would be interesting to determine whether the mechanisms described in our study can also be implemented in chronic IH and more generally in other situations of chronic alterations of physiological parameters leading to adrenal gland activation.

From a pathophysiological point of view, the development of a chronic hypertensive environment in the SHR not only affects the adrenomedullary tissue, but also targets other tissues and organs, leading to alterations in other physiological functions. In this context, the neuroendocrine effects of E on metabolic, behavioural and cognitive status of SHRs are at the forefront [110, 111]. In behavioural tests, the SHR exhibits increased locomotor activity and reduced anxiety [112–115], leading it to be proposed as an animal model for Attention Deficit Hyperactivity Disorder [116]. Learning and memory processes are also modified, due at least in part to increased glucose levels in response to E [117, 118]. As such, chronic arterial hypertension has repercussions on the entire body, threatening its homeostasis. In this context and which can then be considered as a protective mechanism, limiting CA secretion in order not to amplify the hypertensive pathology can take on its full meaning.

Supplementary Information The online version contains supplementary material available at https://doi.org/10.1007/s00018-024-05524-5.

Acknowledgements We thank Drs. Michel G. Desarménien and Philippe Lory for helpful discussion in preparing the manuscript, Drs. Claire Legendre and Hélène Tricoire-Leignel for their technical

advices in the molecular techniques, and Prof. Pascal Richomme for HPLC facility in his laboratory (Univ. Angers, SONAS, SFR QUASAV, Angers, France).

Author contributions V.P., J.P, B.T., J.B., F.D.N., P.F., C.G.-L., C.L. and N.C.G. conducted the experiments. D.B. and D.G. assisted with HPLC equipment. V.P., J.P, B.T., J.B., F.D.N., C.G.-L., C.L. and N.C.G analyzed the data. N.C.G and C.L. designed the experiments. N.C.G. conceived the study and wrote the paper with input from D.H. and C.L.

Funding This work was supported by grants from Centre National de la Recherche Scientifique, Institut National de la Santé et de la Recherche Médicale, Fondation pour la Recherche Médicale (grant INE20100117998), Région Pays de la Loire, Conseil Général de Maine et Loire and Angers Loire Métropole.

Data availability All data generated or analyzed during this study are included in this article and its supplementary information file. The raw data are available upon request from the corresponding author.

Declarations

Ethical approval All animal studies conformed to the animal welfare guidelines of the European Community and were approved by the French Agriculture and Forestry Ministry (authorization numbers/licences 49-2011-18, 49–247, A49007002 and D44015) and by the regional ethic committee (authorization CEEA.2011.12 and APAFIS#2017072117413637).

Consent for publication All authors have approved the content of this manuscript and provided consent for publication.

Competing interests The authors declare no competing interests.

References

1. Tank AW, Lee Wong D (2015) Peripheral and central effects of circulating catecholamines. Compr Physiol 5:1–15. https://doi.org/10.1002/cphy.c140007
2. Johnson MD, Grignolo A, Kuhn CM, Schanberg SM (1983) Hypertension and cardiovascular hypertrophy during chronic catecholamine infusion in rats. Life Sci 33:169–180. https://doi.org/10.1016/0024-3205(83)90410-1
3. Schwartz DD, Eikenburg DC (1986) Cardiovascular responsiveness to sympathetic activation after chronic epinephrine administration. J Pharmacol Exp Ther 238:148–154
4. Fregly MJ, Kikta DC, Threatte RM, Torres JL, Barney CC (1989) Development of hypertension in rats during chronic exposure to cold. J Appl Physiol 66:741–749. https://doi.org/10.1152/jappl.1989.66.2.741
5. Anderson EA, Sinkey CA, Lawton WJ, Mark AL (1989) Elevated sympathetic nerve activity in borderline hypertensive humans. Evidence from direct intraneural recordings. Hypertension 14:177–183. https://doi.org/10.1161/01.hyp.14.2.177
6. Esler M, Ferrier C, Lambert G, Eisenhofer G, Cox H, Jennings G (1991) Biochemical evidence of sympathetic hyperactivity in human hypertension. Hypertension 17:III29–35. https://doi.org/10.1161/01.hyp.17.4_suppl.iii29
7. Papanek PE, Wood CE, Fregly MJ (1991) Role of the sympathetic nervous system in cold-induced hypertension in rats. J Appl Physiol (1985) 71:300–306. https://doi.org/10.1152/jappl.1991.71.1.300
8. Lim DY, Jang SJ, Park DG (2002) Comparison of catecholamine release in the isolated adrenal glands of SHR and WKY rats. Auton Autacoid Pharmacol 22:225–232. https://doi.org/10.1046/j.1474-8673.2002.00264.x
9. Friese RS, Mahboubi P, Mahapatra NR, Mahata SK, Schork NJ, Schmid-Schonbein GW, O'Connor DT (2005) Common genetic mechanisms of blood pressure elevation in two independent rodent models of human essential hypertension. Am J Hypertens 18:633–652. https://doi.org/10.1016/j.amjhyper.2004.11.037
10. Mathar I, Vennekens R, Meissner M, Kees F, Van der Mieren G, Camacho Londono JE, Uhl S, Voets T, Hummel B, van den Bergh A, Herijgers P, Nilius B, Flockerzi V, Schweda F, Freichel M (2010) Increased catecholamine secretion contributes to hypertension in TRPM4-deficient mice. J Clin Invest 120:3267–3279. https://doi.org/10.1172/JCI41348
11. Pak CH (1981) Plasma adrenaline and noradrenaline concentrations of the spontaneously hypertensive rat. Jpn Heart J 22:987–995. https://doi.org/10.1536/ihj.22.987
12. Guerineau NC, Campos P, Le Tissier PR, Hodson DJ, Mollard P (2022) Cell networks in Endocrine/Neuroendocrine gland function. Compr Physiol 12:3371–3415. https://doi.org/10.1002/cphy.c210031
13. Douglas WW (1968) Stimulus-secretion coupling: the concept and clues from chromaffin and other cells. Br J Pharmacol 34:451–474. https://doi.org/10.1111/j.1476-5381.1968.tb08474.x
14. Wakade AR (1981) Studies on secretion of catecholamines evoked by acetylcholine or transmural stimulation of the rat adrenal gland. J Physiol 313:463–480. https://doi.org/10.1113/jphysiol.1981.sp013676
15. Martin AO, Mathieu MN, Chevillard C, Guerineau NC (2001) Gap junctions mediate electrical signaling and ensuing cytosolic Ca2 + increases between chromaffin cells in adrenal slices: a role in catecholamine release. J Neurosci 21:5397–5405. https://doi.org/10.1523/JNEUROSCI.21-15-05397.2001
16. Colomer C, Desarmenien MG, Guerineau NC (2009) Revisiting the stimulus-secretion coupling in the adrenal medulla: role of gap junction-mediated intercellular communication. Mol Neurobiol 40:87–100. https://doi.org/10.1007/s12035-009-8073-0
17. Colomer C, Martin AO, Desarmenien MG, Guerineau NC (2012) Gap junction-mediated intercellular communication in the adrenal medulla: an additional ingredient of stimulus-secretion coupling regulation. Biochim Biophys Acta 1818:1937–1951. https://doi.org/10.1016/j.bbamem.2011.07.034
18. Desarmenien MG, Jourdan C, Toutain B, Vessieres E, Hormuzdi SG, Guerineau NC (2013) Gap junction signalling is a stress-regulated component of adrenal neuroendocrine stimulus-secretion coupling in vivo. Nat Commun 4:2938. https://doi.org/10.1038/ncomms3938
19. Hodson DJ, Legros C, Desarmenien MG, Guerineau NC (2015) Roles of connexins and pannexins in (neuro)endocrine

physiology. Cell Mol Life Sci 72:2911–2928. https://doi.org/10.1007/s00018-015-1967-2
20. Guerineau NC (2018) Gap junction communication between chromaffin cells: the hidden face of adrenal stimulus-secretion coupling. Pflugers Arch 470:89–96. https://doi.org/10.1007/s00424-017-2032-9
21. Guerineau NC (2020) Cholinergic and peptidergic neurotransmission in the adrenal medulla: a dynamic control of stimulus-secretion coupling. IUBMB Life 72:553–567. https://doi.org/10.1002/iub.2117
22. Limas C, Westrum B, Limas CJ (1980) The evolution of vascular changes in the spontaneously hypertensive rat. Am J Pathol 98:357–384
23. Moura E, Afonso J, Serrao MP, Vieira-Coelho MA (2009) Effect of clonidine on tyrosine hydroxylase activity in the adrenal medulla and brain of spontaneously hypertensive rats. Basic Clin Pharmacol Toxicol 104:113–121. https://doi.org/10.1111/j.1742-7843.2008.00339.x
24. Tien LYH, Morgan WH, Cringle SJ, Yu DY (2023) Optimal calculation of Mean pressure from pulse pressure. Am J Hypertens 36:297–305. https://doi.org/10.1093/ajh/hpad026
25. Guerineau NC (2023) Recording of chromaffin cell electrical activity in situ in acute adrenal slices. Methods Mol Biol 2565:113–127. https://doi.org/10.1007/978-1-0716-2671-9_9
26. Almers W, Stanfield PR, Stuhmer W (1983) Lateral distribution of sodium and potassium channels in frog skeletal muscle: measurements with a patch-clamp technique. J Physiol 336:261–284. https://doi.org/10.1113/jphysiol.1983.sp014580
27. Perkins KL (2006) Cell-attached voltage-clamp and current-clamp recording and stimulation techniques in brain slices. J Neurosci Methods 154:1–18. https://doi.org/10.1016/j.jneumeth.2006.02.010
28. Alcami P, Franconville R, Llano I, Marty A (2012) Measuring the firing rate of high-resistance neurons with cell-attached recording. J Neurosci 32:3118–3130. https://doi.org/10.1523/JNEUROSCI.5371-11.2012
29. Chan HL, Lin MA, Wu T, Lee ST, Tsai YT, Chao PK (2008) Detection of neuronal spikes using an adaptive threshold based on the max-min spread sorting method. J Neurosci Methods 172:112–121. https://doi.org/10.1016/j.jneumeth.2008.04.014
30. Milman A, Venteo S, Bossu JL, Fontanaud P, Monteil A, Lory P, Guerineau NC (2021) A sodium background conductance controls the spiking pattern of mouse adrenal chromaffin cells in situ. J Physiol 599:1855–1883. https://doi.org/10.1113/JP281044
31. Colomer C, Olivos-Ore LA, Vincent A, McIntosh JM, Artalejo AR, Guerineau NC (2010) Functional characterization of alpha9-containing cholinergic nicotinic receptors in the rat adrenal medulla: implication in stress-induced functional plasticity. J Neurosci 30:6732–6742. https://doi.org/10.1523/JNEUROSCI.4997-09.2010
32. Barbara JG, Takeda K (1996) Quantal release at a neuronal nicotinic synapse from rat adrenal gland. Proc Natl Acad Sci U S A 93:9905–9909. https://doi.org/10.1073/pnas.93.18.9905
33. Kajiwara R, Sand O, Kidokoro Y, Barish ME, Iijima T (1997) Functional organization of chromaffin cells and cholinergic synaptic transmission in rat adrenal medulla. Jpn J Physiol 47:449–464. https://doi.org/10.2170/jjphysiol.47.449
34. Warashina A, Ogura T (2004) Modeling of stimulation-secretion coupling in a chromaffin cell. Pflugers Arch 448:161–174. https://doi.org/10.1007/s00424-003-1169-x
35. Butterworth E, Jardine BE, Raymond GM, Neal ML, Bassingthwaighte JB (2013) JSim, an open-source modeling system for data analysis. F1000Res 2:288. https://doi.org/10.12688/f1000research.2-288.v1
36. Colomer C, Olivos Ore LA, Coutry N, Mathieu MN, Arthaud S, Fontanaud P, Iankova I, Macari F, Thouennon E, Yon L, Anouar Y, Guerineau NC (2008) Functional remodeling of gap junction-mediated electrical communication between adrenal chromaffin cells in stressed rats. J Neurosci 28:6616–6626. https://doi.org/10.1523/JNEUROSCI.5597-07.2008
37. Schmittgen TD, Livak KJ (2008) Analyzing real-time PCR data by the comparative C(T) method. Nat Protoc 3:1101–1108. https://doi.org/10.1038/nprot.2008.73
38. De Nardi F, Lefort C, Breard D, Richomme P, Legros C, Guerineau NC (2017) Monitoring the secretory behavior of the rat adrenal medulla by high-performance liquid chromatography-based catecholamine assay from slice supernatants. Front Endocrinol (Lausanne) 8:248. https://doi.org/10.3389/fendo.2017.00248
39. Nohta H, Yukizawa T, Ohkura Y, Yoshimura M, Ishida J, Yamaguchi M (1997) Aromatic glycinonitriles and methylamines as pre-column fluorescence derivatization reagents for catecholamines. Anal Chim Acta 344:233–240. https://doi.org/10.1016/S0003-2670(96)00614-9
40. Yoshitake T, Fujino K, Kehr J, Ishida J, Nohta H, Yamaguchi M (2003) Simultaneous determination of norepinephrine, serotonin, and 5-hydroxyindole-3-acetic acid in microdialysis samples from rat brain by microbore column liquid chromatography with fluorescence detection following derivatization with benzylamine. Anal Biochem 312:125–133. https://doi.org/10.1016/s0003-2697(02)00435-9
41. Stroth N, Kuri BA, Mustafa T, Chan SA, Smith CB, Eiden LE (2013) PACAP controls adrenomedullary catecholamine secretion and expression of catecholamine biosynthetic enzymes at high splanchnic nerve firing rates characteristic of stress transduction in male mice. Endocrinology 154:330–339. https://doi.org/10.1210/en.2012-1829
42. Eiden LE, Emery AC, Zhang L, Smith CB (2018) PACAP signaling in stress: insights from the chromaffin cell. Pflugers Arch 470:79–88. https://doi.org/10.1007/s00424-017-2062-3
43. Inoue M, Harada K, Matsuoka H (2020) Mechanisms for pituitary adenylate cyclase-activating polypeptide-induced increase in excitability in guinea-pig and mouse adrenal medullary cells. Eur J Pharmacol 872:172956. https://doi.org/10.1016/j.ejphar.2020.172956
44. Vandael DH, Ottaviani MM, Legros C, Lefort C, Guerineau NC, Allio A, Carabelli V, Carbone E (2015) Reduced availability of voltage-gated sodium channels by depolarization or blockade by tetrodotoxin boosts burst firing and catecholamine release in mouse chromaffin cells. J Physiol 593:905–927. https://doi.org/10.1113/jphysiol.2014.283374
45. Carbone E, Marcantoni A, Giancippoli A, Guido D, Carabelli V (2006) T-type channels-secretion coupling: evidence for a fast low-threshold exocytosis. Pflugers Arch 453:373–383. https://doi.org/10.1007/s00424-006-0100-7
46. Guerineau NC, Desarmenien MG, Carabelli V, Carbone E (2012) Functional chromaffin cell plasticity in response to stress: focus on nicotinic, gap junction, and voltage-gated ca(2+) channels. J Mol Neurosci 48:368–386. https://doi.org/10.1007/s12031-012-9707-7
47. Lingle CJ, Solaro CR, Prakriya M, Ding JP (1996) Calcium-activated potassium channels in adrenal chromaffin cells. Ion Channels 4:261–301. https://doi.org/10.1007/978-1-4899-1775-1_7
48. Martin AO, Mathieu MN, Guerineau NC (2003) Evidence for long-lasting cholinergic control of gap junctional communication between adrenal chromaffin cells. J Neurosci 23:3669–3678. https://doi.org/10.1523/JNEUROSCI.23-09-03669.2003
49. Colomer C, Lafont C, Guerineau NC (2008) Stress-induced intercellular communication remodeling in the rat adrenal medulla. Ann N Y Acad Sci 1148:106–111. https://doi.org/10.1196/annals.1410.040
50. Barbara JG, Poncer JC, McKinney RA, Takeda K (1998) An adrenal slice preparation for the study of chromaffin cells and their

cholinergic innervation. J Neurosci Methods 80:181–189. https://doi.org/10.1016/s0165-0270(97)00200-8
51. Martin AO, Alonso G, Guerineau NC (2005) Agrin mediates a rapid switch from electrical coupling to chemical neurotransmission during synaptogenesis. J Cell Biol 169:503–514. https://doi.org/10.1083/jcb.200411054
52. Hill J, Lee SK, Samasilp P, Smith C (2012) Pituitary adenylate cyclase-activating peptide enhances electrical coupling in the mouse adrenal medulla. Am J Physiol Cell Physiol 303:C257–266. https://doi.org/10.1152/ajpcell.00119.2012
53. Giepmans BN, Moolenaar WH (1998) The gap junction protein connexin43 interacts with the second PDZ domain of the zona occludens-1 protein. Curr Biol 8:931–934. https://doi.org/10.1016/s0960-9822(07)00375-2
54. Marcantoni A, Vandael DH, Mahapatra S, Carabelli V, Sinnegger-Brauns MJ, Striessnig J, Carbone E (2010) Loss of Cav1.3 channels reveals the critical role of L-type and BK channel coupling in pacemaking mouse adrenal chromaffin cells. J Neurosci 30:491–504. https://doi.org/10.1523/JNEUROSCI.4961-09.2010
55. Duan K, Yu X, Zhang C, Zhou Z (2003) Control of secretion by temporal patterns of action potentials in adrenal chromaffin cells. J Neurosci 23:11235–11243. https://doi.org/10.1523/JNEUROSCI.23-35-11235.2003
56. Guerineau NC, Monteil A, Lory P (2021) Sodium background currents in endocrine/neuroendocrine cells: towards unraveling channel identity and contribution in hormone secretion. Front Neuroendocrinol 63:100947. https://doi.org/10.1016/j.yfrne.2021.100947
57. Lingle CJ, Martinez-Espinosa PL, Guarina L, Carbone E (2018) Roles of na(+), ca(2+), and K(+) channels in the generation of repetitive firing and rhythmic bursting in adrenal chromaffin cells. Pflugers Arch 470:39–52. https://doi.org/10.1007/s00424-017-2048-1
58. Vandael DH, Zuccotti A, Striessnig J, Carbone E (2012) Ca(V)1.3-driven SK channel activation regulates pacemaking and spike frequency adaptation in mouse chromaffin cells. J Neurosci 32:16345–16359. https://doi.org/10.1523/JNEUROSCI.3715-12.2012
59. Maruta T, Yanagita T, Matsuo K, Uezono Y, Satoh S, Nemoto T, Yoshikawa N, Kobayashi H, Takasaki M, Wada A (2008) Lysophosphatidic acid-LPA1 receptor-rho-rho kinase-induced up-regulation of Nav1.7 sodium channel mRNA and protein in adrenal chromaffin cells: enhancement of 22Na + influx, 45Ca2 + influx and catecholamine secretion. J Neurochem 105:401–412. https://doi.org/10.1111/j.1471-4159.2007.05143.x
60. Monjaraz E, Navarrete A, Lopez-Santiago LF, Vega AV, Arias-Montano JA, Cota G (2000) L-type calcium channel activity regulates sodium channel levels in rat pituitary GH3 cells. J Physiol 523 Pt 1:45–55. https://doi.org/10.1111/j.1469-7793.2000.00045.x
61. Vega AV, Espinosa JL, Lopez-Dominguez AM, Lopez-Santiago LF, Navarrete A, Cota G (2003) L-type calcium channel activation up-regulates the mRNAs for two different sodium channel alpha subunits (Nav1.2 and Nav1.3) in rat pituitary GH3 cells. Brain Res Mol Brain Res 116:115–125. https://doi.org/10.1016/s0169-328x(03)00279-1
62. Vandael DH, Marcantoni A, Carbone E (2015) Cav1.3 channels as key regulators of Neuron-Like firings and Catecholamine Release in Chromaffin cells. Curr Mol Pharmacol 8:149–161. https://doi.org/10.2174/1874467208666150507105443
63. Black JA, Hoeijmakers JG, Faber CG, Merkies IS, Waxman SG (2013) NaV1.7: stress-induced changes in immunoreactivity within magnocellular neurosecretory neurons of the supraoptic nucleus. Mol Pain 9:39. https://doi.org/10.1186/1744-8069-9-39
64. Monteil A, Guerineau NC, Gil-Nagel A, Parra-Diaz P, Lory P, Senatore A (2023) New insights into the physiology and pathophysiology of the atypical sodium leak channel NALCN. Physiol Rev. https://doi.org/10.1152/physrev.00014.2022
65. Del Castillo J, Katz B (1954) Quantal components of the end-plate potential. J Physiol 124:560–573. https://doi.org/10.1113/jphysiol.1954.sp005129
66. Di Angelantonio S, Matteoni C, Fabbretti E, Nistri A (2003) Molecular biology and electrophysiology of neuronal nicotinic receptors of rat chromaffin cells. Eur J Neurosci 17:2313–2322. https://doi.org/10.1046/j.1460-9568.2003.02669.x
67. Frahm S, Slimak MA, Ferrarese L, Santos-Torres J, Antolin-Fontes B, Auer S, Filkin S, Pons S, Fontaine JF, Tsetlin V, Maskos U, Ibanez-Tallon I (2011) Aversion to nicotine is regulated by the balanced activity of beta4 and alpha5 nicotinic receptor subunits in the medial habenula. Neuron 70:522–535. https://doi.org/10.1016/j.neuron.2011.04.013
68. Wang F, Gerzanich V, Wells GB, Anand R, Peng X, Keyser K, Lindstrom J (1996) Assembly of human neuronal nicotinic receptor alpha5 subunits with alpha3, beta2, and beta4 subunits. J Biol Chem 271:17656–17665. https://doi.org/10.1074/jbc.271.30.17656
69. Gerzanich V, Wang F, Kuryatov A, Lindstrom J (1998) Alpha 5 subunit alters desensitization, pharmacology, ca + + permeability and ca + + modulation of human neuronal alpha 3 nicotinic receptors. J Pharmacol Exp Ther 286:311–320
70. Chavez-Noriega LE, Crona JH, Washburn MS, Urrutia A, Elliott KJ, Johnson EC (1997) Pharmacological characterization of recombinant human neuronal nicotinic acetylcholine receptors h alpha 2 beta 2, h alpha 2 beta 4, h alpha 3 beta 2, h alpha 3 beta 4, h alpha 4 beta 2, h alpha 4 beta 4 and h alpha 7 expressed in Xenopus oocytes. J Pharmacol Exp Ther 280:346–356
71. Mousavi M, Hellstrom-Lindahl E, Guan ZZ, Bednar I, Nordberg A (2001) Expression of nicotinic acetylcholine receptors in human and rat adrenal medulla. Life Sci 70:577–590
72. Arroyo-Jimenez MM, Bourgeois JP, Marubio LM, Le Sourd AM, Ottersen OP, Rinvik E, Fairen A, Changeux JP (1999) Ultrastructural localization of the alpha4-subunit of the neuronal acetylcholine nicotinic receptor in the rat substantia nigra. J Neurosci 19:6475–6487. https://doi.org/10.1523/JNEUROSCI.19-15-06475.1999
73. Scholze P, Huck S (2020) The alpha5 nicotinic acetylcholine receptor subunit differentially modulates alpha4beta2(*) and alpha3beta4(*) receptors. Front Synaptic Neurosci 12:607959. https://doi.org/10.3389/fnsyn.2020.607959
74. Wu J, Liu Q, Yu K, Hu J, Kuo YP, Segerberg M, St John PA, Lukas RJ (2006) Roles of nicotinic acetylcholine receptor beta subunits in function of human alpha4-containing nicotinic receptors. J Physiol 576:103–118. https://doi.org/10.1113/jphysiol.2006.114645
75. Inoue M, Harada K (2023) Enhancement of muscarinic receptor-mediated excitation in spontaneously hypertensive rat adrenal medullary chromaffin cells. Auton Neurosci 248:103108. https://doi.org/10.1016/j.autneu.2023.103108
76. Pereda AE, Curti S, Hoge G, Cachope R, Flores CE, Rash JE (2013) Gap junction-mediated electrical transmission: Regulatory mechanisms and plasticity. Biochim Biophys Acta 1828:134–146. https://doi.org/10.1016/j.bbamem.2012.05.026
77. Guerineau NC (2024) Adaptive remodeling of the stimulus-secretion coupling: lessons from the 'stressed' adrenal medulla. Vitam Horm 124:221–225. https://doi.org/10.1016/bs.vh.2023.05.004
78. Moura E, Pinto CE, Calo A, Serrao MP, Afonso J, Vieira-Coelho MA (2011) Alpha(2)-Adrenoceptor-mediated inhibition of catecholamine release from the adrenal medulla of spontaneously hypertensive rats is preserved in the early stages of hypertension. Basic Clin Pharmacol Toxicol 109:253–260. https://doi.org/10.1111/j.1742-7843.2011.00712.x

79. Tabei R (1966) On histochemical studies of the various organs of spontaneously hypertensive rats. Jpn Circ J 30:717–742. https://doi.org/10.1253/jcj.30.717
80. Ozaki M, Suzuki Y, Yamori Y, Okamoto K (1968) Adrenal catecholamine content in the spontaneously hypertensive rats. Jpn Circ J 32:1367–1372. https://doi.org/10.1253/jcj.32.1367
81. Maruyama T (1969) Electron microscopic studies on the adrenal medulla and adrenal cortex of hypertensive rats. 1. Spontaneously hypertensive rats. Jpn Circ J 33:1271–1284. https://doi.org/10.1253/jcj.33.1271
82. Nagatsu I, Nagatsu T, Mizutani K, Umezawa H, Matsuzaki M, Takeuchi T (1971) Adrenal tyrosine hydroxylase and dopamine beta-hydroxylase in spontaneously hypertensive rats. Nature 230:381–382. https://doi.org/10.1038/230381a0
83. Kumai T, Tanaka M, Watanabe M, Kobayashi S (1994) Elevated tyrosine hydroxylase mRNA levels in the adrenal medulla of spontaneously hypertensive rats. Jpn J Pharmacol 65:367–369. https://doi.org/10.1254/jjp.65.367
84. O'Connor DT, Takiyyuddin MA, Printz MP, Dinh TQ, Barbosa JA, Rozansky DJ, Mahata SK, Wu H, Kennedy BP, Ziegler MG, Wright FA, Schlager G, Parmer RJ (1999) Catecholamine storage vesicle protein expression in genetic hypertension. Blood Press 8:285–295. https://doi.org/10.1080/080370599439508
85. Reja V, Goodchild AK, Phillips JK, Pilowsky PM (2002) Tyrosine hydroxylase gene expression in ventrolateral medulla oblongata of WKY and SHR: a quantitative real-time polymerase chain reaction study. Auton Neurosci 98:79–84. https://doi.org/10.1016/s1566-0702(02)00037-1
86. Reja V, Goodchild AK, Pilowsky PM (2002) Catecholamine-related gene expression correlates with blood pressures in SHR. Hypertension 40:342–347. https://doi.org/10.1161/01.hyp.0000027684.06638.63
87. Moura E, Pinho Costa PM, Moura D, Guimaraes S, Vieira-Coelho MA (2005) Decreased tyrosine hydroxylase activity in the adrenals of spontaneously hypertensive rats. Life Sci 76:2953–2964. https://doi.org/10.1016/j.lfs.2004.11.017
88. Donohue SJ, Stitzel RE, Head RJ (1988) Time Course of Changes in the Norepinephrine content of tissues from spontaneously hypertensive and Wistar Kyoto rats. J Pharmacol Exp Ther 245:24–31
89. Schober M, Howe PR, Sperk G, Fischer-Colbrie R, Winkler H (1989) An increased pool of secretory hormones and peptides in adrenal medulla of stroke-prone spontaneously hypertensive rats. Hypertension 13:469–474. https://doi.org/10.1161/01.hyp.13.5.469
90. Vavrinova A, Behuliak M, Bencze M, Vodicka M, Ergang P, Vaneckova I, Zicha J (2019) Sympathectomy-induced blood pressure reduction in adult normotensive and hypertensive rats is counteracted by enhanced cardiovascular sensitivity to vasoconstrictors. Hypertens Res 42:1872–1882. https://doi.org/10.1038/s41440-019-0319-2
91. Elias S, Delestre C, Courel M, Anouar Y, Montero-Hadjadje M (2010) Chromogranin A as a crucial factor in the sorting of peptide hormones to secretory granules. Cell Mol Neurobiol 30:1189–1195. https://doi.org/10.1007/s10571-010-9595-8
92. Machado JD, Diaz-Vera J, Dominguez N, Alvarez CM, Pardo MR, Borges R (2010) Chromogranins a and B as regulators of vesicle cargo and exocytosis. Cell Mol Neurobiol 30:1181–1187. https://doi.org/10.1007/s10571-010-9584-y
93. Mahapatra NR, O'Connor DT, Vaingankar SM, Hikim AP, Mahata M, Ray S, Staite E, Wu H, Gu Y, Dalton N, Kennedy BP, Ziegler MG, Ross J, Mahata SK (2005) Hypertension from targeted ablation of chromogranin A can be rescued by the human ortholog. J Clin Invest 115:1942–1952. https://doi.org/10.1172/JCI24354
94. Zhang K, Rao F, Rana BK, Gayen JR, Calegari F, King A, Rosa P, Huttner WB, Stridsberg M, Mahata M, Vaingankar S, Mahboubi V, Salem RM, Rodriguez-Flores JL, Fung MM, Smith DW, Schork NJ, Ziegler MG, Taupenot L, Mahata SK, O'Connor DT (2009) Autonomic function in hypertension; role of genetic variation at the catecholamine storage vesicle protein chromogranin B. Circ Cardiovasc Genet 2:46–56. https://doi.org/10.1161/CIRCGENETICS.108.785659
95. Fargali S, Garcia AL, Sadahiro M, Jiang C, Janssen WG, Lin WJ, Cogliani V, Elste A, Mortillo S, Cero C, Veitenheimer B, Graiani G, Pasinetti GM, Mahata SK, Osborn JW, Huntley GW, Phillips GR, Benson DL, Bartolomucci A, Salton SR (2014) The granin VGF promotes genesis of secretory vesicles, and regulates circulating catecholamine levels and blood pressure. FASEB J 28:2120–2133. https://doi.org/10.1096/fj.13-239509
96. Nguyen P, Peltsch H, de Wit J, Crispo J, Ubriaco G, Eibl J, Tai TC (2009) Regulation of the phenylethanolamine N-methyltransferase gene in the adrenal gland of the spontaneous hypertensive rat. Neurosci Lett 461:280–284. https://doi.org/10.1016/j.neulet.2009.06.022
97. Chalmers JP, Howe PR, Wallmann Y, Tumuls I (1981) Adrenaline neurons and PNMT activity in the brain and spinal cord of genetically hypertensive rats and rats with DOCA–salt hypertension. Clin Sci (Lond) 61(Suppl 7):219s–221s. https://doi.org/10.1042/cs061219s
98. Grobecker H, Saavedra JM, Weise VK (1982) Biosynthetic enzyme activities and catecholamines in adrenal glands of genetic and experimental hypertensive rats. Circ Res 50:742–746. https://doi.org/10.1161/01.res.50.5.742
99. Vavrinova A, Behuliak M, Bencze M, Vaneckova I, Zicha J (2019) Which sympathoadrenal abnormalities of adult spontaneously hypertensive rats can be traced to a prehypertensive stage? Hypertens Res 42:949–959. https://doi.org/10.1038/s41440-018-0198-y
100. Lokhandwala MF, Eikenburg DC (1983) Minireview. Presynaptic receptors and alterations in norepinephrine release in spontaneously hypertensive rats. Life Sci 33:1527–1542. https://doi.org/10.1016/0024-3205(83)90693-8
101. Hartmann C, Radermacher P, Wepler M, Nussbaum B (2017) Non-hemodynamic effects of catecholamines. Shock 48:390–400. https://doi.org/10.1097/SHK.0000000000000879
102. Adameova A, Abdellatif Y, Dhalla NS (2009) Role of the excessive amounts of circulating catecholamines and glucocorticoids in stress-induced heart disease. Can J Physiol Pharmacol 87:493–514. https://doi.org/10.1139/y09-042
103. Rubin RP (1969) The metabolic requirements from catecholamine release from the adrenal medulla. J Physiol 202:197–209. https://doi.org/10.1113/jphysiol.1969.sp008804
104. Ushiama S, Ishimaru Y, Narukawa M, Yoshioka M, Kozuka C, Watanabe N, Tsunoda M, Osakabe N, Asakura T, Masuzaki H, Abe K (2016) Catecholamines facilitate fuel expenditure and Protect against Obesity via a Novel Network of the gut-brain Axis in transcription factor skn-1-deficient mice. EBioMedicine 8:60–71. https://doi.org/10.1016/j.ebiom.2016.04.031
105. Kumar GK, Rai V, Sharma SD, Ramakrishnan DP, Peng YJ, Souvannakitti D, Prabhakar NR (2006) Chronic intermittent hypoxia induces hypoxia-evoked catecholamine efflux in adult rat adrenal medulla via oxidative stress. J Physiol 575:229–239. https://doi.org/10.1113/jphysiol.2006.112524
106. Morisawa T (1968) On the noradrenaline reaction of the adrenal medulla in experimental hypertensive rats, especially in spontaneously hypertensive rats. II. Effects of various experimental conditions on the noradrenaline storing cell islets of the adrenal medulla in spontaneouslly hypertensive rats. Jpn Circ J 32:177–193. https://doi.org/10.1253/jcj.32.177

107. Tonshoff C, Hemmick L, Evinger MJ (1997) Pituitary adenylate cyclase activating polypeptide (PACAP) regulates expression of catecholamine biosynthetic enzyme genes in bovine adrenal chromaffin cells. J Mol Neurosci 9:127–140. https://doi.org/10.1007/BF02736856
108. Guerineau NC, Desarmenien MG (2010) Developmental and stress-induced remodeling of cell-cell communication in the adrenal medullary tissue. Cell Mol Neurobiol 30:1425–1431. https://doi.org/10.1007/s10571-010-9583-z
109. Kumar GK, Nanduri J, Peng YJ, Prabhakar NR (2015) Neuromolecular mechanisms mediating the effects of chronic intermittent hypoxia on adrenal medulla. Respir Physiol Neurobiol 209:115–119. https://doi.org/10.1016/j.resp.2015.01.001
110. Gold PE, Stone WS (1988) Neuroendocrine effects on memory in aged rodents and humans. Neurobiol Aging 9:709–717. https://doi.org/10.1016/s0197-4580(88)80136-2
111. Gold PE (2005) Glucose and age-related changes in memory. Neurobiol Aging 26 Suppl 160–64. https://doi.org/10.1016/j.neurobiolaging.2005.09.002
112. Danysz W, Plaznik A, Pucilowski O, Plewako M, Obersztyn M, Kostowski W (1983) Behavioral studies in spontaneously hypertensive rats. Behav Neural Biol 39:22–29. https://doi.org/10.1016/s0163-1047(83)90569-1
113. Soderpalm B (1989) The SHR exhibits less anxiety but increased sensitivity to the anticonflict effect of clonidine compared to normotensive controls. Pharmacol Toxicol 65:381–386. https://doi.org/10.1111/j.1600-0773.1989.tb01193.x
114. Ramos A, Berton O, Mormede P, Chaouloff F (1997) A multiple-test study of anxiety-related behaviours in six inbred rat strains. Behav Brain Res 85:57–69. https://doi.org/10.1016/s0166-4328(96)00164-7
115. Calzavara MB, Lopez GB, Abilio VC, Silva RH, Frussa-Filho R (2004) Role of anxiety levels in memory performance of spontaneously hypertensive rats. Behav Pharmacol 15:545–553. https://doi.org/10.1097/00008877-200412000-00003
116. Meneses A, Perez-Garcia G, Ponce-Lopez T, Tellez R, Gallegos-Cari A, Castillo C (2011) Spontaneously hypertensive rat (SHR) as an animal model for ADHD: a short overview. Rev Neurosci 22:365–371. https://doi.org/10.1515/RNS.2011.024
117. Mori S, Kato M, Fujishima M (1995) Impaired maze learning and cerebral glucose utilization in aged hypertensive rats. Hypertension 25:545–553. https://doi.org/10.1161/01.hyp.25.4.545
118. Grunblatt E, Bartl J, Iuhos DI, Knezovic A, Trkulja V, Riederer P, Walitza S, Salkovic-Petrisic M (2015) Characterization of cognitive deficits in spontaneously hypertensive rats, accompanied by brain insulin receptor dysfunction. J Mol Psychiatry 3:6. https://doi.org/10.1186/s40303-015-0012-6